

skin samples were analyzed by histological examinations. Application of DMBA-TPA to mouse skin resulted in a significant increase in epidermal thickness (Figure 3A) and number of infiltrated leukocytes (Figure 3B), as well as induction of the epidermal proliferative marker PCNA (Figure 3C and D) by 1.4-, 3.6- and 2.8-fold as compared with the vehicle ( $P < 0.001$ ). Of interest, 13-HOA at a dose of 1600 nmol significantly suppressed the increases in epidermal thickness by 28% ( $P < 0.001$ ), number of infiltrated leukocytes by 76% ( $P < 0.001$ ) and induction of PCNA by 59% ( $P < 0.001$ ) (Figure 3A-D). Even at the lowest dose (160 nmol), 13-HOA significantly reduced the number of leukocytes and induction of PCNA by 41% ( $P < 0.001$ ) and 38% ( $P < 0.001$ ), respectively (Figure 3B-D). The PCNA score for the DMBA-only group tended to be higher than that for the non-treated control, which was inconsistent with our other preliminary results (T. Tanaka and A. Murakami, unpublished data). At this moment, we have no clear explanation for this discrepancy, though other proliferation assays (e.g. Ki-67) might resolve the contradiction.

*13-HOA inhibited TPA-induced transformation of JB6 P+ cells*

Subsequently, the effects of 13-HOA on TPA-induced transformation of JB6 P+ cells were evaluated. HOA (40  $\mu$ M), NS-398 (100  $\mu$ M) and LA (100  $\mu$ M) did not significantly affect cell viability after 24 h

incubation or the rate of spontaneous transformation after 14 days. Vehicle-treated control cells had  $11.0 \pm 10.2$  anchorage-independent colonies/dish after 14 days, whereas the addition of TPA increased the number by 15.8-fold ( $P < 0.001$ ) (Figure 4A). 13-HOA at 8 and 40  $\mu$ M decreased the relative rate of TPA-induced colony formation by 70 and 100%, respectively ( $P < 0.001$ ). In addition, NS-398, used as a positive control (23), at 40 and 100  $\mu$ M inhibited the rate by 80–100% ( $P < 0.001$ ), whereas LA was inactive, even at a concentration of 100  $\mu$ M.

*13-HOA attenuated TPA-induced AP-1 transactivation but not ERK1/2 phosphorylation*

Since 13-HOA markedly inhibited TPA-induced ear inflammation, skin tumor promotion and *in vitro* transformation, we examined its effects on AP-1 transactivation and an MAPK pathway to address underlying molecular mechanisms. ERK1/2 have been reported to be the most important protein kinase of the MAPK family, and previous studies have suggested that resultant AP-1 transactivation is required for TPA-induced JB6 P+ cell transformation (7,24,25).

As shown in Figure 4B, TPA-treated JB6 P<sup>+</sup> cells increased AP-1 transactivation level by 2.7-fold at 12 h ( $P < 0.005$ ), and pretreatment with 13-HOA (40  $\mu$ M) for 30 min ( $P < 0.005$ ) and NS-398

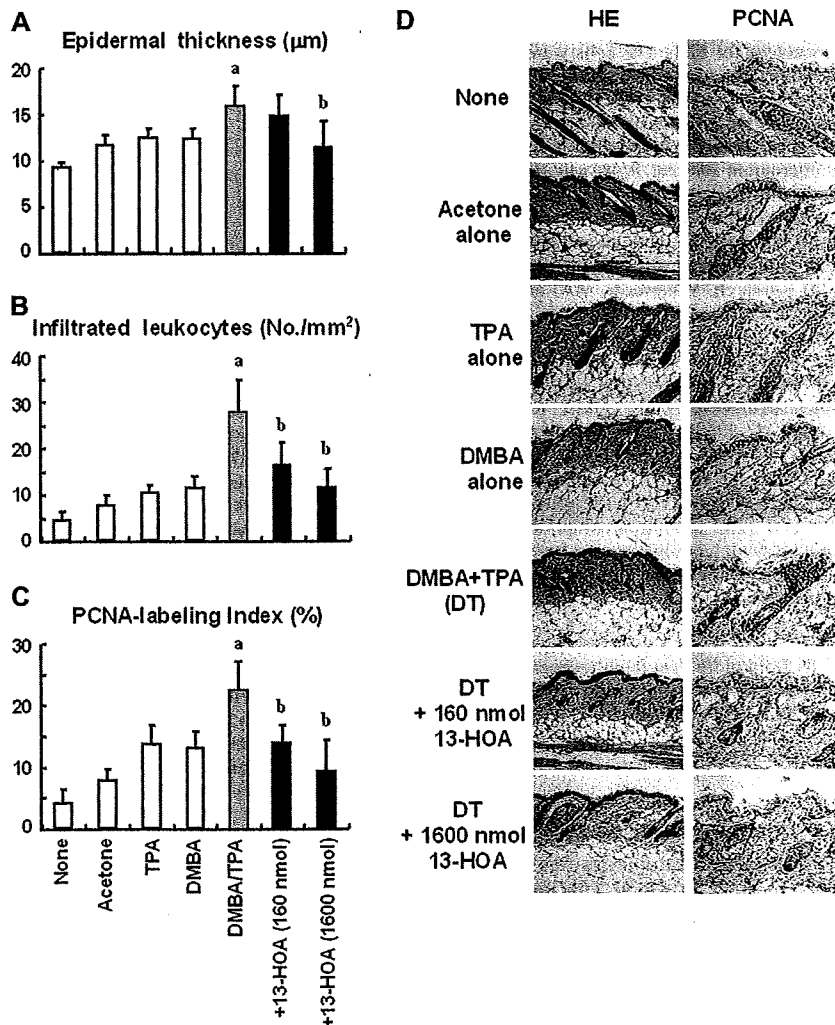


**Fig. 3.** After week 20 of the two-stage mouse skin carcinogenesis experiment, randomly selected biopsy samples from 12 mice in the none, acetone, TPA-only and DMBA-only groups and from 18 mice in the DMBA-TPA, +160 nmol 13-HOA and +1600 nmol 13-HOA groups were subjected to histopathological analysis to determine epidermal thickness (A), numbers of infiltrated leukocytes (B) and PCNA-labeling index (C and D). Representative histological results of mouse skin from each group after staining with hematoxylin and eosin (HE; original magnification  $\times 10$ ), and PCNA immunohistochemistry results (original magnification  $\times 20$ ) are shown in (D). Student's *t*-test was used to determine significant differences. <sup>a</sup> $P < 0.001$  versus acetone, <sup>b</sup> $P < 0.001$  versus DMBA-TPA.

(100  $\mu\text{M}$ ) also suppressed TPA-induced AP-1 transactivation by 31% ( $P < 0.05$ ). However, both 13-HOA and LA did not affect TPA-upregulated ERK1/2 phosphorylation, whereas NS-398 slightly potentiated it (Figure 4C).

#### 13-HOA induced *pdcd4* JB6 P+ cells and mouse skin

The above results led us to explore novel molecules associated with tumor promotion. Expression of the novel tumor suppressor *Pdcd4* was shown to suppress TPA-mediated tumor promotion in mouse skin and transformation of JB6 cell lines via inhibition of AP-1 mediated transcription (12,13,26). On the other hand, *Pdcd4* had no effect on the phosphorylation of ERK1/2 (27,28). For these reasons, we hypoth-

esized that the effects of 13-HOA on TPA-induced inflammation, tumor promotion and transformation may be related to induction of *Pdcd4*. To test this hypothesis, we investigated the time course (0–9 h) of *pdcd4* mRNA expression in JB6 P+ cells treated with the vehicle or 13-HOA (40  $\mu\text{M}$ ), in the presence or absence of TPA (Figure 5A). 13-HOA was found to transiently increase the level of *pdcd4* mRNA expression, which reached a maximum after 6 h. Then, 13-HOA treatment for 6 h induced it by 2.1-fold ( $P < 0.05$ ) without TPA and by 2.5-fold ( $P < 0.05$ ) with TPA. Although NS-398 (100  $\mu\text{M}$ ) and 13-HOA (8  $\mu\text{M}$ ) also tended to upregulate *pdcd4* mRNA, the increase was not statistically significant, whereas 13-HOA (1.6  $\mu\text{M}$ ) and LA (100  $\mu\text{M}$ ) had no effects (data not shown).

Of note, treatment with 13-HOA for 6 h restored TPA-decreased *Pdcd4* protein in JB6 P+ cells ( $P < 0.05$ ) (Figure 5B). Neither NS-398 (100  $\mu\text{M}$ ) nor LA (100  $\mu\text{M}$ ) induced *Pdcd4* protein (data not shown). Topical application of TPA (8 nmol) to ICR mouse skin significantly decreased *Pdcd4* protein expression at 6 h ( $P < 0.05$ ),

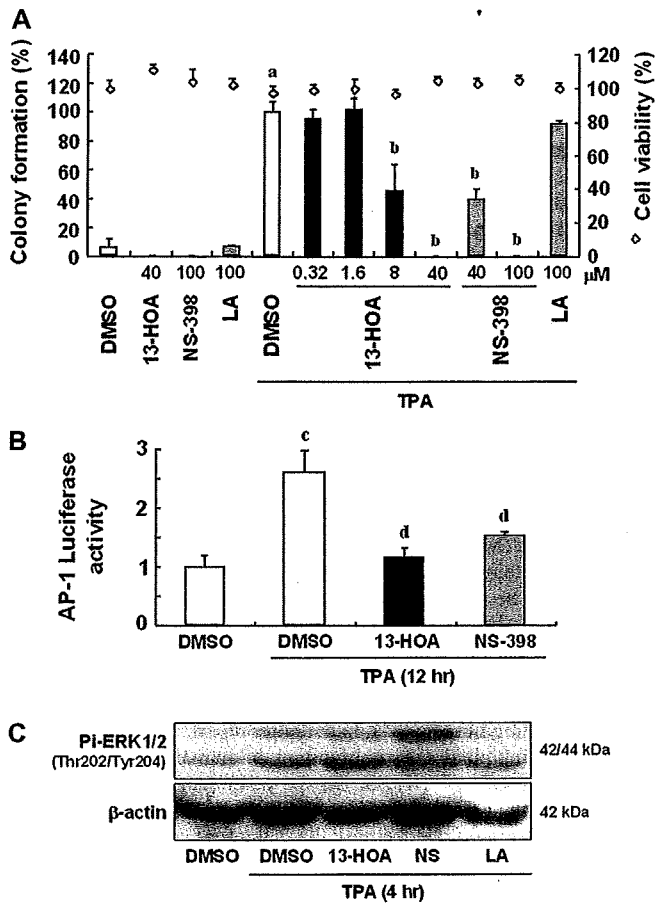


**Fig. 4.** 13-HOA inhibited TPA-induced transformation and AP-1 activation but not ERK1/2 phosphorylation in JB6 P+ cells. (A) JB6 P+ cells were exposed to TPA (30 nM) with DMSO, 13-HOA (0.32, 1.6, 8 or 40  $\mu\text{M}$ ), NS-398 (40  $\mu\text{M}$ ) or LA (100  $\mu\text{M}$ ) on 0.33% soft agar medium. Following a 14 day incubation in a  $\text{CO}_2$  incubator at 37°C, the number of TPA-induced anchorage-independent colonies was  $174.5 \pm 13.6$  per 3000 cells. Each bar represents the mean obtained from triplicate dishes. Treatment with the compounds for 24 h did not affect cellular viability. Each value is the mean of triplicate wells  $\pm$  SD. Student's *t*-test was used to determine significant differences. <sup>a</sup> $P < 0.001$  versus DMSO, <sup>b</sup> $P < 0.001$  versus TPA + DMSO. (B) For report gene assay, AP-1-luciferase reporter plasmid stable transfectant JB6 P+<sup>11</sup> cells were cultured with DMSO, 13-HOA (40  $\mu\text{M}$ ) or NS-398 (100  $\mu\text{M}$ ) for 30 min before treatment with or without TPA (30 nM). The luciferase activity was measured 12 h later. The data are expressed by mean  $\pm$  SD from triplicate experiments. A Student's *t*-test was used to determine significant differences. <sup>c</sup> $P < 0.005$  versus DMSO, <sup>d</sup> $P < 0.005$  versus TPA + DMSO. (C) JB6 P+ cells were incubated with DMSO, HOA (40  $\mu\text{M}$ ), NS-398 (100  $\mu\text{M}$ ) and LA (100  $\mu\text{M}$ ) for 30 min and then treated with TPA (30 nM) for 4 h. Western blotting was performed as described in Materials and Methods, and  $\beta$ -actin was used as the internal control. The result is representative of three independent experiments.

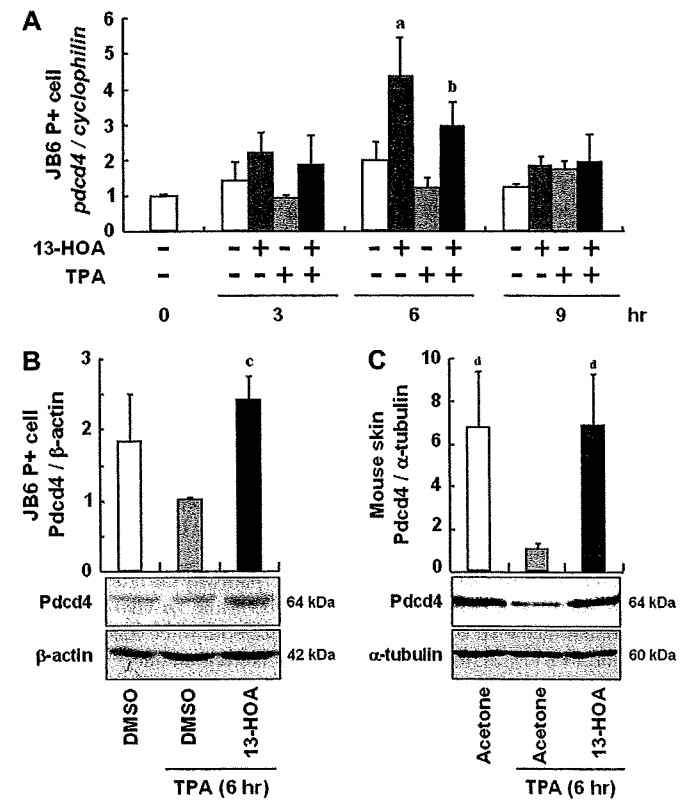


**Fig. 5.** 13-HOA induced *Pdcd4* mRNA and protein in JB6 P+ cells and mouse skin. (A) Cells were incubated with DMSO or 13-HOA (40  $\mu\text{M}$ ) for 30 min and then the cells were treated with or without TPA (30 nM). Total RNA was isolated from cells at the time points as indicated. The mRNA expression of *cyclophilin* was used as the internal standard. Each value represents the mean  $\pm$  SD of three to four separate experiments. To determine significant differences, Student's *t*-test was used. <sup>a</sup> $P < 0.05$  versus DMSO (6 h), <sup>b</sup> $P < 0.05$  versus TPA + DMSO (6 h). (B) Cells were treated with DMSO or 13-HOA (40  $\mu\text{M}$ ) before treatment with or without TPA (30 nM) for 6 h. The data represent the mean  $\pm$  SD of three separate experiments, and a representative picture is shown. A Student's *t*-test was used to determine significant differences. <sup>c</sup> $P < 0.05$  versus TPA + DMSO (6 h). (C) Acetone or 13-HOA (1600 nmol) was applied to shaved dorsal skin of ICR mice. After 20 min, TPA (8 nmol) was applied to the same area. After 6 h, the mice were killed and epidermis of each mouse was collected. The expression of  $\alpha$ -tubulin was used as the internal standard. Results are expressed as the mean  $\pm$  SD of three experiments, and the picture is a representative of those experiments. Statistical analysis was done by Student's *t*-test. <sup>d</sup> $P < 0.05$  versus TPA + acetone.

whereas 13-HOA (1600 nmol) pretreatment 20 min before TPA treatment completely blocked it ( $P < 0.05$ ).

## Discussion

The functional link between inflammation and cancer has been supported by experimental results showing that tumor promotion occurs following exposure of cells to chemical irritants such as TPA, which is a strong inducer of inflammatory reactions (4). In this study, we examined the anti-inflammatory and antitumor-promoting activities of 13-HOA using an assay of TPA-induced acute inflammation in mouse ears as well as a two-stage mouse skin carcinogenesis model. Our findings clearly indicated that 13-HOA, but not LA, significantly inhibited TPA-induced ear edema formation and mouse skin tumor promotion (Figures 2 and 3). These results are partly supported by Ha *et al.* (29), who also demonstrated that LA had no inhibitory effect on chemically induced mouse skin carcinogenesis. Meanwhile, a protein kinase C inhibitor, staurosporine, inhibited DMBA–teleocidin-induced skin cancer, whereas it promoted tumor formation in DMBA-initiated mouse skin in the absence of another tumor promoter (30). In the present study, repetitive treatments with 13-HOA resulted in no tumors in DMBA-initiated mouse skin (Figure 2) and 13-HOA did not increase the rate of spontaneous transformation in JB6 P+ cells (Figure 4A), suggesting that 13-HOA does not act as a tumor promoter. Furthermore, our histological analyses revealed that 13-HOA significantly inhibited the infiltration of proinflammatory leukocytes (Figure 3B), which may have some relevance to our previous findings that 13-HOA markedly suppressed the expression of several proinflammatory mRNAs in LPS-stimulated RAW 264.7 macrophages (18) and TPA-treated THP-1 monocytic cells (T.Nishizawa and A.Murakami, unpublished data).

It is notable that 13-HOA inhibited TPA-induced JB6 P+ transformation in a concentration-dependent manner (Figure 4A), whereas LA had no effects. These results are consistent with those in the present ear inflammation (Figure 2A) and skin tumor promotion (Figure 2B–D) assays. 13-HOA (40  $\mu$ M) and NS-398 (100  $\mu$ M) abolished TPA-induced colony formation. That may be due to something other than cytotoxicity, since significant cell viability was maintained during the 24 h incubation period (Figure 4A). Liu *et al.* (31) reported that a dietary fatty acid, docosahexanoic acid, inhibited TPA-induced transformation of JB6 P+ cells by ~62% at a concentration of 60  $\mu$ M, thus it is suggested that the suppressive potency of 13-HOA is greater than that of docosahexanoic acid.

Dhar *et al.* noted the MAPKs–AP-1 pathway is critical for TPA-induced transformation of JB6 P+ cells, while *in vivo* results using dominant-negative c-Jun-expressing transgenic mice also revealed its importance (7,32). In addition, both fos-like region antigen (Fra-1) and JunD are essential components of the TPA-activated AP-1 complex, and ERK-dependent activation of Fra-1 is required for AP-1 transactivation in JB6 P+ cells (33,34). On the other hand, our previous study demonstrated that 13-HOA inhibits the LPS-induced AP-1 transactivation and phosphorylation of ERK1/2 in RAW 264.7 cells (18), and in the present study, 13-HOA suppressed TPA-induced AP-1 transactivation as well (Figure 4B). To our surprise, however, 13-HOA did not inhibit, whereas NS-398, a selective cyclooxygenase-2 inhibitor, slightly activated TPA-induced ERK1/2 activation in JB6 P+ cells (Figure 4C). Although it was previously reported that TPA activated c-Jun N-terminal kinase (JNK)1/2, p38 and c-Jun in JB6 P+ cells (35), analysis of time-course (TPA treatment for 1–12 h) phosphorylation of JNK1/2, p38 and c-Jun by western blotting did not reveal any detectable changes under the present experimental conditions, and 13-HOA had no effects on those (data not shown). Huang *et al.* (36) showed that dominant-negative JNK had no effect on TPA-induced colony formation by JB6 P+ cells and Liu *et al.* (37) reported that AP-1 was activated through a molecular mechanism not associated with TPA-activated JNK1/2. Moreover, JNK activation is required for tumor necrosis factor- $\alpha$  but not TPA-induced transformation, whereas ERK activation plays an essential role in TPA-induced transformation of JB6 P+ cells (36). Based on our and these other results, it may be possible to rule out the possibility

that suppression of JNK1/2, p38 and c-Jun is involved in the inhibitory mechanisms of transformation by 13-HOA.

There is a growing body of evidence that Pdc4 has several key roles in antitumor promotion. Jansen *et al.* (13) reported that transgenic mice overexpressing Pdc4 in the epidermis showed significant reductions in tumor promotion, whereas Yang *et al.* (12,26) noted that an elevated expression of Pdc4 inhibited tumor promotion of JB6 P+ cells induced by TPA and tumorigenic JB6 RT101 (Tx) cells. In the present study, 13-HOA (40  $\mu$ M) did not have an effect on ERK1/2 phosphorylation (Figure 4C), thus we hypothesized that 13-HOA may induce Pdc4 expression resulting in inhibition of TPA-induced transformation in JB6 P+ cells. Treatment of JB6 P+ cells with 13-HOA (40  $\mu$ M) induced *pdc4* mRNA expression in a transient manner (Figure 5A). NS-398 (100  $\mu$ M) suppressed TPA-induced AP-1 activation but not ERK1/2 phosphorylation (Figure 4B and C), and Zhang *et al.* (14) reported that NS-398 induced *pdc4* mRNA using differential screening of colon carcinoma cells, whereas its effect was not remarkable with the JB6 P+ cells in our study (data not shown). Although we examined *pdc4* mRNA inducibility using several food factors known to suppress tumor promotion in mouse skin (38–41), none showed significant effects on *pdc4* mRNA expression (data not shown). Pdc4 protein was also induced by 13-HOA (40  $\mu$ M and 1600 nmol) in JB6 P+ cells and mouse skin treated with TPA, whereas TPA reduced Pdc4 protein expression (Figure 5B and C). Recently, Matsushashi *et al.* (42) showed an inverse correlation between PCNA expression and Pdc4 expression in the human skin, and Yang *et al.* (27) reported that Pdc4 inhibited extracellular matrix protease activity and cell migration in RKO human colon carcinoma cells. Thus, it might be possible that the induction of Pdc4 by 13-HOA resulted in the inhibition of TPA-induced increases in leukocytes infiltration and PCNA (Figure 3B–D). Although the roles of Pdc4 in inflammation are not clear, Pdc4 inhibited constitutively or induced AP-1 activation (12), suggesting its potential for the prevention of inflammation in which AP-1 activation plays a major role. In fact, LPS reduced Pdc4 expression in both mRNA and protein level in RAW 264.7 mouse macrophage (M.Yasuda and A.Murakami, unpublished data). Thus, it is probably that the inhibition by 13-HOA of TPA-induced ear inflammation may be associated with putative Pdc4 induction. To our knowledge, this is the first report of a natural product being able to induce Pdc4 expression. Lipoxin A, one of the lipoxygenase products of arachidonic acid, showed broad anti-inflammatory activities (43) and inhibited proliferation of human lung fibroblasts in experimental models of lung fibrosis (44). In the latter report, Wu *et al.* reported that lipoxin A inhibited the proliferation of human lung fibroblasts via upregulation of p27 (Kip1). On the other hand, Ozpolat *et al.* (15) showed that knockdown of Pdc4 by RNA interference downregulated p27 in acute myeloid leukemia cells. Therefore, it could be possible that lipoxin A might induce p27 through upregulation of Pdc4.

Yang *et al.* reported that Fra-1- and JunD-induced AP-1 activation was inhibited by Pdc4 expression in a concentration-dependent manner. Furthermore, Pdc4 had no interaction with AP-1 proteins either directly or indirectly, thus it is considered to regulate a mediator that controls AP-1 transactivation in JB6 P+ cells (12). Identification of a still unknown Pdc4-binding protein using a proteomics approach and analysis of the effects of 13-HOA on regulation of that protein are crucial for elucidating how 13-HOA inhibits TPA-induced AP-1 activity, as well as how induction of Pdc4 by 13-HOA contributes to the suppression of neoplastic transformation. These issues are now under investigation and the results may be reported elsewhere.

Phosphatidylinositolide 3-kinase/Akt/mammalian target of rapamycin pathway was reported to negatively regulate *pdc4* mRNA expression in human acute promyelocytic cells (15), while the *pdc4* gene was previously detected as a target of the transcription factor *v-myb* myeloblastosis viral oncogene homolog (Myb) in a number of different hematopoietic avian cell lineages (45). On the other hand, Pdc4 translation was partially regulated by microRNA-21 (miR-21) in breast and colorectal cancer cells (46), and AP-1 (c-Jun, JunB and Fra-1) induced miR-21 expression, followed by downregulation of Pdc4 expression, which was included in a positive autoregulation

loop with AP-1, miR-21 and Pdc4 as a negative regulator of AP-1 in a rat thyroid cell system (47). Furthermore, Chen *et al.* (48) hypothesized that Myb may be a target of miR-21. Also the stability of Pdc4 protein is controlled by an ubiquitination-dependent mechanism associated with protein kinase C-dependent phosphatidylinositol 3-kinase/Akt/mammalian target of rapamycin and MEK-ERK pathways (49,50). Thus, the expression processes of Pdc4 are regulated in a complicated multistep manner. Meanwhile, 13-HOA suppressed AP-1 activity in the present study (Figure 4B). Therefore, we consider that 13-HOA may negatively regulate miR-21 and positively regulate Myb in JB6 P+ cells. Additional clarification of the molecular mechanisms involved in JB6 P+ cells as well as other cell lines and examination of the role of 13-HOA with those mechanisms are necessary. Those are now in progress in our laboratory.

In conclusion, our results suggest that 13-HOA is a novel food factor with anti-inflammatory and chemopreventive properties. Since efficient separation and purification methods of 13-HOA have been established (17), multiple evaluations of its cancer preventive efficacy may be feasible. It suppressed TPA-induced AP-1 activation but not ERK1/2 activation. Of interest, 13-HOA was found to induce the expression of the novel transformation suppressor Pdc4 mRNA and protein both *in vitro* and *in vivo*. On the other hand, we could not clarify whether the inhibitory effects of 13-HOA on TPA-induced *in vitro* and *in vivo* activities are dependent on Pdc4 induction. Additional studies are necessary to understand the action mechanisms of this unique fatty acid.

#### Funding

Grant-in-Aid for Cancer Research from the Ministry of Health, Labor and Welfare of Japan (A.M. and T.T.).

#### Acknowledgements

We thank Yasushi Nishikawa and Kazuo Uenakai of Research Center Tamanoi Vinegar, Co. Ltd for providing us with 13-HOA.

*Conflict of Interest Statement:* None declared.

#### References

- Naito, M. *et al.* (1989) Genetic background and development of skin tumors. *Carcinog. Compr. Surv.*, **11**, 187–212.
- Yuspa, S. (1994) The pathogenesis of squamous cell cancer: lessons learned from studies of skin carcinogenesis—thirty-third G.H.A. Clowes Memorial Award Lecture. *Cancer Res.*, **54**, 1178–1189.
- DiGiovanni, J. *et al.* (1994) Role of the epidermal growth factor receptor and transforming growth factor alpha in mouse skin carcinogenesis. *Prog. Clin. Biol. Res.*, **387**, 113–138.
- Mueller, M. (2006) Inflammation in epithelial skin tumours: old stories and new ideas. *Eur. J. Cancer*, **42**, 735–744.
- Colburn, N. *et al.* (1979) Tumour promoter induces anchorage independence irreversibly. *Nature*, **281**, 589–591.
- Bernstein, L. *et al.* (1989) AP1/jun function is differentially induced in promotion-sensitive and resistant JB6 cells. *Science*, **244**, 566–569.
- Dhar, A. *et al.* (2002) The role of AP-1, NF-kappaB and ROS/NOS in skin carcinogenesis: the JB6 model is predictive. *Mol. Cell. Biochem.*, **234–235**, 185–193.
- Ma, C. *et al.* (2007) The role of glycogen synthase kinase 3beta in the transformation of epidermal cells. *Cancer Res.*, **67**, 7756–7764.
- Shibahara, K. *et al.* (1995) Isolation of a novel mouse gene MA-3 that is induced upon programmed cell death. *Gene*, **166**, 297–301.
- Göke, A. *et al.* (2002) DUG is a novel homologue of translation initiation factor 4G that binds eIF4A. *Biochem. Biophys. Res. Commun.*, **297**, 78–82.
- Cmarik, J. *et al.* (1999) Differentially expressed protein Pdc4 inhibits tumor promoter-induced neoplastic transformation. *Proc. Natl Acad. Sci. USA*, **96**, 14037–14042.
- Yang, H. *et al.* (2001) A novel transformation suppressor, Pdc4, inhibits AP-1 transactivation but not NF-kappaB or ODC transactivation. *Oncogene*, **20**, 669–676.
- Jansen, A. *et al.* (2005) Epidermal expression of the translation inhibitor programmed cell death 4 suppresses tumorigenesis. *Cancer Res.*, **65**, 6034–6041.
- Zhang, Z. *et al.* (2001) Detection of differentially expressed genes in human colon carcinoma cells treated with a selective COX-2 inhibitor. *Oncogene*, **20**, 4450–4456.
- Ozpolat, B. *et al.* (2007) Programmed cell death-4 tumor suppressor protein contributes to retinoic acid-induced terminal granulocytic differentiation of human myeloid leukemia cells. *Mol. Cancer Res.*, **5**, 95–108.
- Hayashi, Y. *et al.* (1996) A new cytotoxic compound from a water extract of corn. *Biosci. Biotechnol. Biochem.*, **60**, 1115–1117.
- Kuga, H. *et al.* (1993) Isolation and characterization of cytotoxic compounds from corn. *Biosci. Biotechnol. Biochem.*, **57**, 1020–1021.
- Murakami, A. *et al.* (2005) New class of linoleic acid metabolites biosynthesized by corn and rice lipoxygenases: suppression of proinflammatory mediator expression via attenuation of MAPK- and Akt-, but not PPARgamma-, dependent pathways in stimulated macrophages. *Biochem. Pharmacol.*, **70**, 1330–1342.
- Lin, S. *et al.* (2003) Rhein inhibits TPA-induced activator protein-1 activation and cell transformation by blocking the JNK-dependent pathway. *Int. J. Oncol.*, **22**, 829–833.
- Murakami, A. *et al.* (1992) Chalcone tetramers, lophirachalcone and alatachalcone, from *Lophira alata* as possible anti-tumor promoters. *Biosci. Biotechnol. Biochem.*, **56**, 769–772.
- Murakami, A. *et al.* (2000) Inhibitory effect of citrus nobletin on phorbol ester-induced skin inflammation, oxidative stress, and tumor promotion in mice. *Cancer Res.*, **60**, 5059–5066.
- Chang, P. *et al.* (2003) Osteopontin induction is required for tumor promoter-induced transformation of preneoplastic mouse cells. *Carcinogenesis*, **24**, 1749–1758.
- Liu, G. *et al.* (2003) NS-398 and piroxicam suppress UVB-induced activator protein 1 activity by mechanisms independent of cyclooxygenase-2. *J. Biol. Chem.*, **278**, 2124–2130.
- Watts, R. *et al.* (1998) Expression of dominant negative Erk2 inhibits AP-1 transactivation and neoplastic transformation. *Oncogene*, **17**, 3493–3498.
- Huang, C. *et al.* (1998) Shortage of mitogen-activated protein kinase is responsible for resistance to AP-1 transactivation and transformation in mouse JB6 cells. *Proc. Natl Acad. Sci. USA*, **95**, 156–161.
- Yang, H. *et al.* (2003) Pdc4 suppresses tumor phenotype in JB6 cells by inhibiting AP-1 transactivation. *Oncogene*, **22**, 3712–3720.
- Yang, H. *et al.* (2006) Tumorigenesis suppressor Pdc4 down-regulates mitogen-activated protein kinase kinase kinase 1 expression to suppress colon carcinoma cell invasion. *Mol. Cell. Biol.*, **26**, 1297–1306.
- Wang, Q. *et al.* (2008) Downregulation of tumor suppressor Pdc4 promotes invasion and activates both beta-catenin/Tcf and AP-1-dependent transcription in colon carcinoma cells. *Oncogene*, **27**, 1527–1535.
- Ha, Y. *et al.* (1987) Anticarcinogens from fried ground beef: heat-altered derivatives of linoleic acid. *Carcinogenesis*, **8**, 1881–1887.
- Yoshizawa, S. *et al.* (1990) Tumor-promoting activity of staurosporine, a protein kinase inhibitor on mouse skin. *Cancer Res.*, **50**, 4974–4978.
- Liu, G. *et al.* (2001) Omega 3 but not omega 6 fatty acids inhibit AP-1 activity and cell transformation in JB6 cells. *Proc. Natl Acad. Sci. USA*, **98**, 7510–7515.
- Young, M. *et al.* (1999) Transgenic mice demonstrate AP-1 (activator protein-1) transactivation is required for tumor promotion. *Proc. Natl Acad. Sci. USA*, **96**, 9827–9832.
- Young, M. *et al.* (2002) Transactivation of Fra-1 and consequent activation of AP-1 occur extracellular signal-regulated kinase dependently. *Mol. Cell. Biol.*, **22**, 587–598.
- Bernstein, L. *et al.* (1999) Tumor promotion resistant cells are deficient in AP-1 DNA binding, JunD DNA binding and JunD expression and form different AP-1-DNA complexes than promotion sensitive cells. *Biochim. Biophys. Acta*, **1489**, 263–280.
- Hou, D. *et al.* (2004) Anthocyanidins inhibit activator protein 1 activity and cell transformation: structure-activity relationship and molecular mechanisms. *Carcinogenesis*, **25**, 29–36.
- Huang, C. *et al.* (1999) JNK activation is required for JB6 cell transformation induced by tumor necrosis factor-alpha but not by 12-O-tetradecanoylphorbol-13-acetate. *J. Biol. Chem.*, **274**, 29672–29676.
- Liu, G. *et al.* (2001) Two novel glycosides from the fruits of *Morinda citrifolia* (noni) inhibit AP-1 transactivation and cell transformation in the mouse epidermal JB6 cell line. *Cancer Res.*, **61**, 5749–5756.
- Nishino, H. *et al.* (2004) Cancer prevention by antioxidants. *Biofactors*, **22**, 57–61.

39. Murakami, A. *et al.* (2004) Zerumbone, a sesquiterpene in subtropical ginger, suppresses skin tumor initiation and promotion stages in ICR mice. *Int. J. Cancer*, **110**, 481–490.
40. Murakami, A. *et al.* (1996) 1'-Acetoxychavicol acetate, a superoxide anion generation inhibitor, potently inhibits tumor promotion by 12-O-tetradecanoylphorbol-13-acetate in ICR mouse skin. *Oncology*, **53**, 386–391.
41. Nakamura, Y. *et al.* (1998) Suppression of tumor promoter-induced oxidative stress and inflammatory responses in mouse skin by a superoxide generation inhibitor 1'-acetoxychavicol acetate. *Cancer Res.*, **58**, 4832–4839.
42. Matsuhashi, S. *et al.* (2007) Expression patterns of programmed cell death 4 protein in normal human skin and some representative skin lesions. *Exp. Dermatol.*, **16**, 179–184.
43. Bannenberg, G. *et al.* (2004) Lipoxins and novel 15-epi-lipoxin analogs display potent anti-inflammatory actions after oral administration. *Br. J. Pharmacol.*, **143**, 43–52.
44. Wu, S. *et al.* (2006) Lipoxin A4 inhibits proliferation of human lung fibroblasts induced by connective tissue growth factor. *Am. J. Respir. Cell Mol. Biol.*, **34**, 65–72.
45. Appl, H. *et al.* (2002) Targeted disruption of c-myc in the chicken pre B-cell line DT40. *Oncogene*, **21**, 3076–3081.
46. Asangani, I. *et al.* (2007) MicroRNA-21 (miR-21) post-transcriptionally downregulates tumor suppressor Pcd4 and stimulates invasion, intravasation and metastasis in colorectal cancer. *Oncogene*, **27**, 2128–2136.
47. Talotta, F. *et al.* (2009) An autoregulatory loop mediated by miR-21 and PDCD4 controls the AP-1 activity in RAS transformation. *Oncogene*, **28**, 73–84.
48. Chen, A. *et al.* (2008) Complementary analysis of microRNA and mRNA expression during phorbol 12-myristate 13-acetate (TPA)-induced differentiation of HL-60 cells. *Biotechnol. Lett.*, **30**, 2045–2052.
49. Dorrello, N. *et al.* (2006) S6K1- and betaTRCP-mediated degradation of PDCD4 promotes protein translation and cell growth. *Science*, **314**, 467–471.
50. Schmid, T. *et al.* (2008) Translation inhibitor Pcd4 is targeted for degradation during tumor promotion. *Cancer Res.*, **68**, 1254–1260.

Received January 22, 2009; revised April 15, 2009; accepted April 25, 2009



## Original Article

# Protein expression analysis of inflammation-related colon carcinogenesis

Yumiko Yasui, Takuji Tanaka\*

Department of Oncologic Pathology, Kanazawa Medical University, 1-1 Daigaku, Uchinada, Ishikawa 920-0293, Japan

Dr. Takuji Tanaka, Department of Oncologic Pathology, Kanazawa Medical University, 1-1 Daigaku, Uchinada, Ishikawa 920-0293, Japan.

E-mail: takutt@kanazawa-med.ac.jp

\*Corresponding author

Published: 02 June, 2009

Journal of Carcinogenesis 2009, 8:10

DOI: 10.4103/1477-3163.51851

Received: 03 March, 2009

Accepted: 20 April, 2009

This article is available from: <http://www.carcinogenesis.com/content/8/1/10>

© 2009 Tanaka,

## Abstract

**Background:** Chronic inflammation is a risk factor for colorectal cancer (CRC) development. The aim of this study was to determine the differences in protein expression between CRC and the surrounding nontumorous colonic tissues in the mice that received azoxymethane (AOM) and dextran sodium sulfate (DSS) using a proteomic analysis. **Materials and Methods:** Male ICR mice were given a single intraperitoneal injection of AOM (10 mg/kg body weight), followed by 2% (w/v) DSS in their drinking water for seven days, starting one week after the AOM injection. Colonic adenocarcinoma developed after 20 weeks and a proteomics analysis based on two-dimensional gel electrophoresis and ultraflex TOF/TOF mass spectrometry was conducted in the cancerous and nontumorous tissue specimens. **Results:** The proteomic analysis revealed 21 differentially expressed proteins in the cancerous tissues in comparison to the nontumorous tissues. There were five markedly increased proteins (beta-tropomyosin, tropomyosin 1 alpha isoform b, S100 calcium binding protein A9, and an unknown protein) and 16 markedly decreased proteins (Car1 proteins, selenium-binding protein 1, HMG-CoA synthase, thioredoxin 1, 1 Cys peroxiredoxin protein 2, Fcgbp protein, Cytochrome c oxidase, subunit Va, ETHE1 protein, and 7 unknown proteins). **Conclusions:** There were 21 differentially expressed proteins in the cancerous tissues of the mice that received AOM and DSS. Their functions include metabolism, the antioxidant system, oxidative stress, mucin production, and inflammation. These findings may provide new insights into the mechanisms of inflammation-related colon carcinogenesis and the establishment of novel therapies and preventative strategies to treat carcinogenesis in the inflamed colon.

**Keywords:** Colitis-related carcinogenesis, mice, proteomics analysis

## INTRODUCTION

Patients with chronic inflammatory bowel disease (IBD) including ulcerative colitis (UC) are at increased risk of developing colorectal cancer (CRC).<sup>[1-4]</sup> Indeed, IBD ranks among the top three high-risk conditions for CRC, together with familial adenomatous polyposis (FAP) and hereditary nonpolyposis colorectal cancer (HNPCC).<sup>[5]</sup> While the latter two hereditary diseases have a well-understood genetic

etiology, CRC development in association with IBD appears to be closely related to chronic inflammation of the large bowel mucosa. Also, IBD-associated colon carcinogenesis can be summarized as an inflammation-dysplasia-carcinoma sequence: hyperplastic lesions in the inflamed mucosa develop CRC through flat dysplasia.<sup>[6,7]</sup>

An azoxymethane (AOM)/dextran sodium sulfate (DSS) mouse model<sup>[8]</sup> was used to investigate the changes in global

gene expression in the background of inflammation-related colon cancer.<sup>[9]</sup> A comprehensive DNA microarray analysis revealed that a number of genes altered their expression in the colonic mucosa of mice exposed to AOM/DSS and their expression was significantly increased or decreased in comparison to those found in the mice given AOM or DSS alone.<sup>[9]</sup> The number of genes with altered expression in the colonic mucosa of the mice that received AOM/DSS at week 5 was greater than that detected at week 10.<sup>[9]</sup> These genes showing their striking altered expression included *Wif1*, *Plat*, *Myc*, *Plscr2*, *Pparbp*, *Tgfb3*, and *Pparg*.<sup>[9]</sup>

Comparative proteomic analyses have been used for identifying proteins critical for phenotypic changes that occur during disease development.<sup>[10]</sup> A reproducible correlation is found between the expression patterns of multiple proteins within epithelial cells and the progression of neoplasms in a variety of tissues, such as the oral cavity,<sup>[11]</sup> prostate,<sup>[12]</sup> lung,<sup>[13,14]</sup> mammary gland,<sup>[15]</sup> liver,<sup>[16]</sup> and colon.<sup>[17]</sup> Yeo *et al.*<sup>[18]</sup> recently reported that a total of 38 proteins are differentially expressed in colonic tumors and normal mucosa of female C57BL/6 mice that received cycle treatment with DSS. They also stressed the importance of reduced expression of transgelin among the proteins as a biomarker of colitis-related colon carcinogenesis. However, they did not use a colonic carcinogen combined with DSS, rather they used a utilized cycle treatment with DSS to induce CRC in the inflamed colon.

The current study analyzed a number of proteins to isolate and identify tumor specific proteins that might be involved in the development of colitis-related CRC in AOM/DSS model mice<sup>[9]</sup> by two-dimensional gel electrophoresis to further investigate the protein expression during colitis-associated carcinogenesis.

## MATERIALS AND METHODS

### Animal experiments

#### Animals, chemicals, and diets

Male Crj: CD-1 (ICR) mice (Charles River Japan, Inc., Tokyo) aged five weeks were used in this study. AOM was purchased from Sigma-Aldrich Co. (St. Louis, MO, USA). DSS with a molecular weight of 36,000–50,000 (Cat. No. 160110) was obtained from MP Biomedicals, LLC (Aurora, OH, USA). DSS for the induction of colitis was dissolved in distilled water at a concentration of 2% (w/v). Charles River Formula (CRF)-1 (Oriental Yeast Co., Ltd., Tokyo, Japan) was used as a basal diet throughout the study.

#### Experimental procedure

After arriving, mice were acclimated for seven days with tap

water and a pelleted basal diet of CRF-1, ad libitum. They received a single intraperitoneal (i.p.) injection of 10 mg/kg body weight AOM. Starting one week after the AOM injection, the animals were exposed to 2% DSS in the drinking water for seven days, and then were followed without any further treatment until the experiment was done. They were sacrificed by CO<sub>2</sub> euthanasia at week 20 for the analysis. All mice were maintained at the Kanazawa Medical University Animal Facility according to the Institutional Animal Care Guidelines and were maintained under controlled conditions of humidity (50±10%), light (12/12 hr light/dark cycle), and temperature (23±2°C). The study protocol was approved by the Ethical Committee for animal experimentation of the Kanazawa Medical University.

### Two-dimensional (2-D) gel electrophoresis

#### Chemicals

The sources for chemicals and materials used in the present study were: 3-([3-Cholamidopropyl]-dimethylammonio)-1-propanesulfonate (CHAPS) from Wako Pure Chemicals (Osaka, Japan), N-decyl-N,N-dimethyl-3-ammonio-1-propane-sulfonate (SB3-10) from Sigma-Aldrich, ampholine from GE Healthcare UK Ltd. (Amersham Place, Little Chalfont, Buckinghamshire HP7 9NA, England), and all other chemicals were purchased from Wako Pure Chemicals.

#### 2-D polyacrylamide gel electrophoresis (PAGE)

Colonic tumors (histologically confirmed as well-differentiated tubular adenocarcinomas) and nontumorous mucosa tissues were collected from the mice that received AOM and DSS and were stored at -80°C prior to use. The frozen tissues were homogenized with five volumes of lysis buffer (5 M urea, 2 M thiourea, 2% CHAPS, 2% SB3-10, 1% dithiothreitol, and 2% ampholine). The protein concentration of these samples was measured using a Protein Assay Kit (Bio-Rad Laboratories). The samples (100 µg) were applied overnight to Immobiline Drystrip (GE Healthcare Bio-Science) by in-gel rehydration.<sup>[19,20]</sup> The rehydrated gels were then gently dried with tissue paper to remove excess fluid and isoelectric focusing (IEF) was performed in a Multiphor II electrophoresis chamber (GE Healthcare Bio-Science) according to the manufacturer's instructions. Second dimension SDS-PAGE was performed in 9–18% acrylamide gradient gels using an IsoDalt electrophoresis chamber (GE Healthcare Bio-Science). The 2-D gels were stained with SYPRO Ruby (Bio-Rad Laboratories) under the manufacturer's protocols.<sup>[21]</sup> The SYPRO Ruby stained proteins were detected using the Molecular Imager FX (Bio-Rad Laboratories) and were subjected to in-gel digestion. Image analyses and database management were carried out using the ImageMaster 2D Platinum image analysis software program (GE Healthcare Bio-Science).

**In-gel digestion and mass spectrometric identification of proteins**  
Protein spots were excised from the 2-D gels using clean scalpels, and were washed twice with Milli-Q water, and dehydrated in 100% acetonitrile (ACN) until they turned opaque white. The spots were then dried in a vacuum centrifuge, and subsequently rehydrated in 10  $\mu$ l of digestion solution consisting of 50 mM  $\text{NH}_4\text{HCO}_3$ , 5 mM  $\text{CaCl}_2$ , 0.01  $\mu\text{g}/\mu\text{l}$  modified sequence-grade trypsin (Promega Co., Ltd.). After incubation for 16 hr at 37°C the digestion was terminated by adding 10  $\mu$ l of 5% trifluoroacetic acid (TFA). The peptides were extracted three times for 20 mins with 50  $\mu$ l of 5% TFA, 50% ACN, and the extracts were pooled and dried in a vacuum centrifuge. The dried materials were resuspended with 10  $\mu$ l of 0.1% TFA. To remove excess salts from the extracts, solid-phase extraction was performed using  $\text{C}_{18}$  ZipTip (Millipore Co., Ltd.) according to the manufacturer's instructions. The peptides were eluted from the ZipTip by 3  $\mu$ l of 50% ACN, 0.1% TFA and 1  $\mu$ l of the eluants were spotted onto a target plate. Then, the spots on the target plate were immediately mixed with 0.5  $\mu$ l of a matrix solution containing 0.3 mg/ml  $\alpha$ -cyano-hydroxycinnamic acid, 33% acetone, 66% ethanol, and were completely air-dried at room temperature. MS and MS/MS spectra were

obtained using an Ultraflex TOF/TOF mass spectrometer (Bruker Daltonics Co., Ltd.). An external peptide mixture was used to calibrate the instrument. Identification of proteins was carried out using the MASCOT software (Matrix Science Inc.) with the NCBI nr database.

## RESULTS

A comparative proteomic analysis was conducted on tumors or nontumorous mucosa specimens using 2-DE and MALDI-TOF. We identified 21 spots showing a more than 3.0-fold increase [Figure 1] or decrease [Figure 2] in density in the cancerous tissues. Following trypsin digestion, each spot was analyzed by MALDI-TOF MS, 4 [Table 1] and 9 [Table 2] proteins could be identified.

The proteins with an increased expression in the cancerous tissues were beta-tropomyosin (8.41-fold increase), tropomyosin 1 alpha isoform b (7.28-fold increase), S100 calcium binding protein A9 (calgranulin B, 3.78-fold increase), peptidylprolylisomerase A (3.43-fold increase), and an unknown protein product (6.47-fold increase: Table 1). The proteins with decreased expression in the cancerous

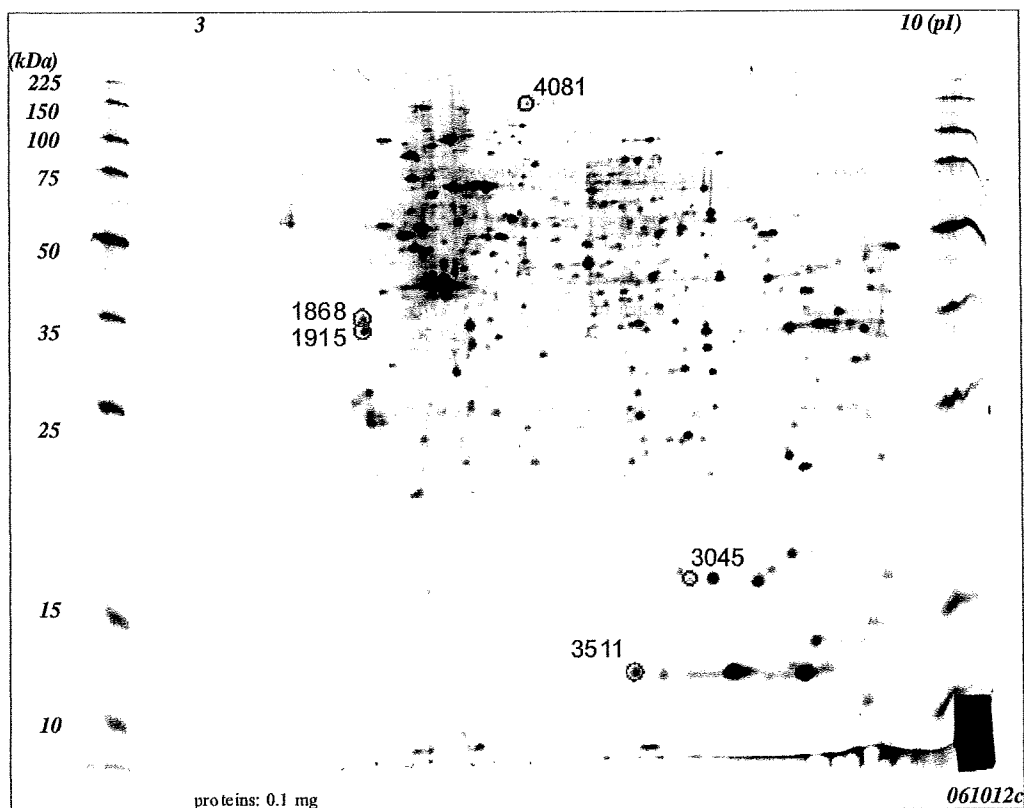


**Figure 1:** Two dimensional electrophoretic patterns of the whole cell proteins obtained from the cancerous tissues of the mice that received AOM/DSS. The gel was silver stained. The protein spots identified in this study are all circled.

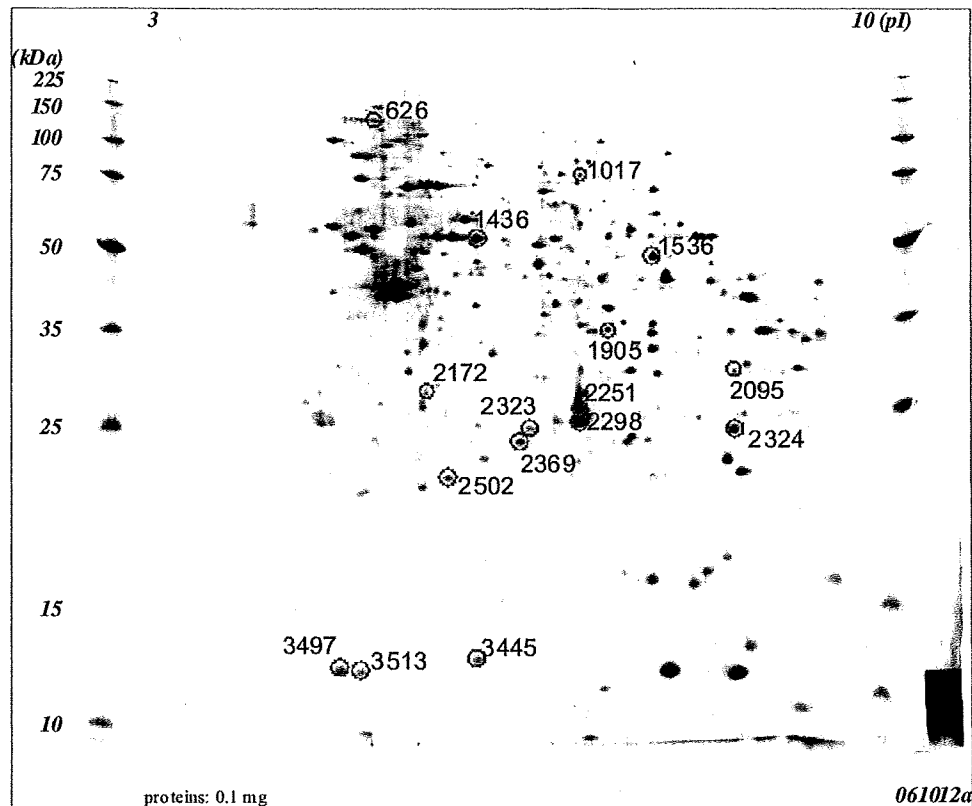


**Figure 2: Two dimensional electrophoretic patterns of whole cell proteins obtained from the inflamed colonic mucosa without any tumors in the mice that received AOM/DSS. Gel was silver stained. The protein spots identified in this study are all circle.**

**Table 1: Proteins that showed increased expression in the cancerous tissues of mice**

Spot no.	Description	Fold change	pI	MW (Da)	Accession no.
1915	beta-tropomyosin	8.41	4.61	32982	gil50190
1868	tropomyosin 1, alpha isoform b	7.28	4.71	32746	gil78000190
4081	-	6.47	-	-	N. D.
3511	S100 calcium binding protein A9 (calgranulin B)	3.78	6.64	13211	gil6677837
3045	Peptidylprolyl isomerase A	3.43	7.74	18131	gil53237015

**Table 2: Proteins that showed decreased expression in the cancerous tissues of mice**

Spot no.	Description	Fold change	pI	MW (Da)	Accession no.
2172	-	-28.57	-	-	N. D.
2095	-	-18.73	-	-	N. D.
2298	Car1 protein	-17.08	6.44	28370	gil15029975
1436	Selenium-binding protein 1 (56 kDa selenium-binding protein)	-7.39	5.97	52889	gil134259
3445	-	-6.23	-	-	N. D.
2251	Car1 protein	-5.45	6.44	28370	gil15029975
1536	HMG CoA synthase	-5.39	7.69	48384	gil555835
1905	-	-5.14	-	-	N. D.
3497	Thioredoxin 1	-4.77	4.80	12010	gil14789654
2369	1-Cys peroxiredoxin protein 2	-4.49	5.71	24999	gil3789944
2502	-	-3.64	-	-	N. D.
626	Fcgbp protein	-3.45	5.35	72499	gil74179916
3513	Cytochrome c oxidase, subunit Va	-3.38	6.08	16248	gil6680986
2324	-	-3.36	-	-	N. D.
1017	-	-3.14	-	-	N. D.
2323	ETHE1 protein	-3.09	6.78	28234	gil12963539

tissues were constitutive androstane receptor 1 (Car1) protein (17.08-fold decrease for spot 2298 and 5.45-fold decrease for spot 2251), Selenium-binding protein 1 (SELENBP1, 56 kDa selenium-binding protein, 7.39-fold decrease), 3-hydroxy-3-methylglutaryl coenzyme A (HMG CoA) synthase (5.39-fold decrease), thioredoxin 1 (4.77-fold decrease), 1-cys peroxiredoxin protein 2 (4.49-fold decrease), fcgbp protein (3.45-fold decrease), cytochrome c oxidase, subunit Va (3.38-fold decrease), and ETHE1 protein (3.09-fold decrease; Table 2). Seven other unknown proteins were also identified to show a decreased expression in the cancerous tissues [Table 2].

## DISCUSSION

A comparative proteome analysis of CRC induced by AOM/DSS and the nontumorous mucosa revealed that a total of 21 demonstrated proteins (5 increased and 16 decreased expressions) altered their expression in the cancerous tissues in comparison to the nontumorous tissues. The number of proteins with altered expression was much smaller than genes that showed differential expression patterns in the previous DNA microarray analysis.<sup>[9]</sup> The proteins that showed altered expression in this study were not consistent with those reported by Yeo *et al.*<sup>[18]</sup> This discrepancy may be due to the differences of experimental designs between the two studies.

Car1 showed a 17.08-fold decrease for spot 2298 and 5.45-fold decrease for spot 2251 in the cancerous tissue in comparison to the nontumorous tissue. The constitutive androstane receptor (CAR, MB67NR1I3) is a member of the nuclear receptor (NR) superfamily.<sup>[22]</sup> The expression is most prevalent in the liver, where it mediates the induction of drug and endobiotic metabolism through a mechanism involving the direct regulation of genes encoding biotransformation enzymes.<sup>[23,24]</sup> Specifically, CAR targets include genes encoding phase I and phase II drug metabolizing functions as well as drug transport genes.<sup>[25]</sup> The nuclear pregnane X receptor (PXR) and CAR play central roles in protecting the body against environmental xenobiotics.<sup>[26]</sup> PXR and CAR are activated by a wide range of xenobiotics and regulate cytochrome P450 (CYP) and other genes whose products are involved in the detoxification of these chemicals. Using microarray analyses, a number of CAR-regulated genes have been elucidated,<sup>[26]</sup> and many of these seem to be directly involved in the metabolism and transport of xenobiotics.<sup>[27,28]</sup> The expression of many genes involved in xenobiotic/drug metabolism and transport are regulated by at least three nuclear receptors or xenosensors: CAR, PXR, and aryl hydrocarbon receptor. These receptors establish crosstalk with other nuclear receptors or transcription factors controlling signaling pathways that regulate the homeostasis of bile acids, lipids,

glucose, inflammation, vitamins, hormones, and others. In the CYP profiles of colon carcinogenesis, significantly higher levels of several CYPs, such as CYP1B1, CYP2S1, CYP2U1, CYP3A5, and CYP51 are present in primary CRC, while CYP3A4 is the most frequently expressed in the normal colon.<sup>[29]</sup> However, CYP 3A expression is altered in the experimental colitis.<sup>[30]</sup> While the role of CYPs in IBD is not known, NR is involved in the mediation of inflammatory processes and therefore may play a role in the development of IBD.<sup>[31,32]</sup> In fact, a significant down-regulation of PXR and the PXR target gene, MDR1, is observed in healthy mucosa adjacent to diseased colonic and terminal ileum of patients with CD and UC.<sup>[32]</sup> Transgenic mice that do not express the MDR1 gene spontaneously develop colitis under specific pathogen-free conditions and the pathological picture of the colon is quite similar to severe intestinal inflammation observed in IBD.<sup>[31]</sup> The finding that the expression of CAR1 protein markedly decreased in the cancerous tissue in this study suggests that the decreasing expression of CAR1 protein causes down-regulation of the expression of the metabolism and transport of xenobiotics, such as CYP3A4 or MDR1. The comprehensive DNA microarray analysis using colonic mucosa of AOM/DSS treated and untreated mice,<sup>[9]</sup> revealed that certain CYP families (CYP2d26, CYP4f16, and CYP2c55) was down-regulated in the colonic mucosa of mice that received AOM/DSS. Thus, CYP may play an important role of the inflammation-related colon carcinogenesis.

HMG-CoA synthase demonstrated a 5.39-fold decrease in the cancerous tissue in this study. HMG-CoA synthase catalyzes a committed step in the pathways for isoprenoid, cholesterol, and ketone body production.<sup>[33]</sup> Cytosolic HMG-CoA synthase, mainly associated with the production of cholesterol and isoprenoid, is expressed in many tissues and it has a negative feedback mechanism with the accumulation of intracellular cholesterol, which is partly regulated by sterol-regulatory element-binding protein (SREBP),<sup>[34]</sup> the same as HMG-CoA reductase. Recently, a HMG-CoA reductase inhibitor is reported to activate the transcription of cytosolic HMG-CoA synthase via SREBP.<sup>[35]</sup> Dietary pitavastatin inhibited AOM/DSS-induced colon carcinogenesis in our previous study,<sup>[36]</sup> suggesting that HMG-CoA synthase is involved in inflammation-related colon carcinogenesis. On the other hand, mitochondrial HMG-CoA synthase, in which is associated with the production of ketone, is mainly expressed in the liver and intestine. Fasting, cAMP, and fatty acids increase its transcriptional rate, while refeeding and insulin repress the rate.<sup>[37]</sup> Unlikely cytosolic HMG-CoA synthase, mitochondrial HMG-CoA synthase is regulated by peroxisomal proliferators regulatory element (PPRE), but not SREBP. The regulation of mitochondrial

HMG-CoA synthase gene expression by fatty acids is mediated through PPRE, to which peroxisome proliferators activated receptor (PPAR) can bind.<sup>[38]</sup> PPAR is involved in colorectal oncogenesis.<sup>[39]</sup> Previously, we reported that dietary administration of ligands for PPAR $\gamma$  and  $\alpha$  effectively suppressed the development of colonic epithelial malignancies induced by AOM/DSS in female ICR mice.<sup>[40]</sup>

The current study showed that Thioredoxin-1 (Trx), a 12kDa protein, was down-regulated by 4.77-fold in the cancerous tissues. This protein is located in the cytoplasm and when translocated into the nucleus has antioxidative and redox-regulating functions. Oxidative stress can be defined as the imbalance between cellular oxidant species production and antioxidant capability. Reactive oxygen species (ROS) are involved in a variety of different cellular processes ranging from apoptosis and necrosis to cell proliferation and carcinogenesis.<sup>[41,42]</sup> Intracellular Trx regulates DNA binding of several transcription factors including p53, nuclear factor (NF)- $\kappa$ B, and activator protein (AP)-1.<sup>[42]</sup> In our previous studies, NF- $\kappa$ B is highly expressed in colonic cancer induced by AOM/DSS and certain modulatory agents of its expression inhibit CRC development in the inflamed colon.<sup>[41,43,44]</sup> In addition, circulating Trx inhibits neutrophil infiltration into the sites of inflammation.<sup>[45]</sup> These findings suggest that Trx thus plays an important role, not only as an antioxidant and anti-apoptotic molecule, but also as an anti-inflammatory molecule. Therefore, Trx can be a good marker for oxidative stress in various diseases.<sup>[46-48]</sup> Recently, serum Trx level was reported to be significantly higher in IBD patients and its levels correlated with disease activity.<sup>[49]</sup> Trx-overexpressing transgenic mice show a decreased severity of colitis in mice treated with DSS.<sup>[49]</sup> Moreover, the administration of recombinant human Trx decreases the severity of colonic inflammation in interleukin (IL)-10 KO mice.<sup>[49]</sup> These findings strongly suggest that Trx is involved in the pathophysiology of IBD. Alteration of Trx expression is involved in colitis-related carcinogenesis via regulating DNA binding activity of several transcription factors, including p53, NF- $\kappa$ B, and AP-1 or gene expression associated with inflammation or apoptosis. The other proteins which showed decreased expression in the tumor tissue included Selenium-binding protein 1, HMG CoA synthase, 1-Cys peroxiredoxin protein 2, Fcgbp protein, Cytochrome c oxidase, subunit Va, and ETHE1 protein.

We also observed that the proteins showed highly increased expression in the tumor tissue. The expression of  $\beta$ -tropomyosin and tropomyosin 1 were highly increased by 8.41-fold (spot no. 1915) and 7.28-fold (spot no. 1868), respectively, in the cancer tissue in comparison to the nontumorous tissue. Tropomyosin (TM) is an actin-binding

protein, which is localized head to tail along the length of the actin filament and controls cell motility.<sup>[50]</sup> Although the role of TMs in muscle contraction is well known, their role in nonmuscle cells is less clear. Several lines of evidence suggest that high molecular weight (HMW) TMs encoded by TPM-1 ( $\alpha$ -TM) and TPM-2 ( $\beta$ -TM) genes<sup>[51]</sup> may contribute to the tumor suppressor activity of TGF- $\beta$ .<sup>[52]</sup> Bakin *et al.*<sup>[52]</sup> reported that induction of TMs and stress fibers play an essential role in TGF- $\beta$ -control of cell motility, and the loss of this TGF- $\beta$ -response is a critical step in the acquisition of a metastatic phenotype by tumor cells. TMs are involved in pathogenesis of IBD, UC, and CD,<sup>[53-55]</sup> although the role in colitis-related colon oncogenesis is not known. Other proteins that were highly expressed in the tumor tissue were S100 calcium binding protein A9 and Peptidylprolyl isomerase A.

In conclusion, the proteomes of CRC and that of nontumorous mucosa of mice that received AOM and DSS were compared in gels, and differentially expressed proteins were identified by mass spectrometry. A total of 13 proteins from 21 spots were identified by 2-DE and MALDI-TOF MS. Among 13 proteins which showed different expression, CAR1, a member of nuclear receptor superfamily, may play an especially important role in this carcinogenesis model as it showed the most drastic decrease. The study of the protein expression in the tumor tissue and nontumorous mucosa in colitis-associated cancer of a mice model (AOM/DSS model) may help us to find tumor-specific proteins for understanding the pathogenesis of colitis-associated cancer development. Proteomic technologies can thus be used to design rational drugs according to the molecular profile of the cancer cells, and thereby facilitate the development of personalized cancer therapy and prevention.

## CONCLUSIONS

There were 21 proteins differently expressed in the cancerous tissues of mice that received AOM and DSS. Their functions included metabolism, the antioxidant system, oxidative stress, mucin production, and inflammation. This is the first report describing a comprehensive protein expression analysis in an AOM/DSS-induced mouse colon carcinogenesis model. These findings may provide new insights into the mechanisms of inflammation-related colon carcinogenesis and the establishment of novel therapies and preventative strategies against carcinogenesis in inflamed colonic tissue.

## REFERENCES

1. Hussain SP, Hofseth LJ, Harris CC. Radical causes of cancer. *Nat Rev Cancer* 2003; 3:276-85.
2. Lashner BA, Provencher KS, Bozdech JM, Brzezinski A. Worsening risk for the development of dysplasia or cancer in patients with chronic ulcerative

- colitis. *Am J Gastroenterol* 1995;90:377-80.
3. Miyamoto S, Yasui Y, Murakami A, Tanaka T. Molecular mechanism of colorectal carcinogenesis. In: Tanaka T, editor. *Cancer: Disease Progression and Chemoprevention Kerala (India): Research Signpost*; 2007. p. 45-56.
  4. Yasui Y, Kim M, Oyama T, Tanaka T. Colorectal carcinogenesis and suppression of tumor development by inhibition of enzymes and molecular targets. *Curr Enzyme Inhibition* 2009;5:1-26.
  5. Itzkowitz SH, Yio X. Inflammation and cancer IV. Colorectal cancer in inflammatory bowel disease: The role of inflammation. *Am J Physiol Gastrointest Liver Physiol* 2004; 287:G7-17.
  6. Xie J, Itzkowitz SH. Cancer in inflammatory bowel disease. *World J Gastroenterol* 2008;14:378-89.
  7. Zisman TL, Rubin DT. Colorectal cancer and dysplasia in inflammatory bowel disease. *World J Gastroenterol* 2008;14:2662-9.
  8. Tanaka T, Kohno H, Suzuki R, Yamada Y, Sugie S, Mori H. A novel inflammation-related mouse colon carcinogenesis model induced by azoxymethane and dextran sodium sulfate. *Cancer Sci* 2003;94:965-73.
  9. Suzuki R, Miyamoto S, Yasui Y, Sugie S, Tanaka T. Global gene expression analysis of the mouse colonic mucosa treated with azoxymethane and dextran sodium sulfate. *BMC Cancer* 2007;7:84.
  10. Hanash SM. Global profiling of gene expression in cancer using genomics and proteomics. *Curr Opin Mol Ther* 2001;3:538-45.
  11. Hu S, Wong DT. Oral cancer proteomics. *Curr Opin Mol Ther* 2007;9:467-76.
  12. Meehan KL, Holland JW, Dawkins HJ. Proteomic analysis of normal and malignant prostate tissue to identify novel proteins lost in cancer. *Prostate* 2002;50:54-63.
  13. Brichory F, Beer D, Le Naour F, Giordano T, Hanash S. Proteomics-based identification of protein gene product 9.5 as a tumor antigen that induces a humoral immune response in lung cancer. *Cancer Res* 2001;61:7908-12.
  14. Oh JM, Brichory F, Puravs E, Kuick R, Wood C, Rouillard JM, et al. A database of protein expression in lung cancer. *Proteomics* 2001;1:1303-19.
  15. Wulfkuhle JD, McLean KC, Pawletz CP, Sgroi DC, Trock BJ, Steeg PS, et al. New approaches to proteomic analysis of breast cancer. *Proteomics* 2001;1:1205-15.
  16. Sun W, Xing B, Sun Y, Du X, Lu M, Hao C, et al. Proteome analysis of hepatocellular carcinoma by two-dimensional difference gel electrophoresis: novel protein markers in hepatocellular carcinoma tissues. *Mol Cell Proteomics* 2007;6:1798-808.
  17. Ahmed FE. Molecular markers that predict response to colon cancer therapy. *Expert Rev Mol Diagn* 2005;5:353-75.
  18. Yeo M, Kim DK, Park HJ, Oh TY, Kim JH, Cho SW, et al. Loss of transgelin in repeated bouts of ulcerative colitis-induced colon carcinogenesis. *Proteomics* 2006;6:1158-65.
  19. Sanchez JC, Rouge V, Pisteu M, Ravier F, Tonella L, Moosmayer M, et al. Improved and simplified in-gel sample application using reswelling of dry immobilized pH gradients. *Electrophoresis* 1997;18:324-7.
  20. Rabilloud T, Valette C, Lawrence JJ. Sample application by in-gel rehydration improves the resolution of two-dimensional electrophoresis with immobilized pH gradients in the first dimension. *Electrophoresis* 1994;15:1552-8.
  21. Lopez MF, Berggren K, Chernokalskaya E, Lazarev A, Robinson M, Patton WF. A comparison of silver stain and SYPRO Ruby Protein Gel Stain with respect to protein detection in two-dimensional gels and identification by peptide mass profiling. *Electrophoresis* 2000;21:3673-83.
  22. Chawla A, Repa JJ, Evans RM, Mangelsdorf DJ. Nuclear receptors and lipid physiology: opening the X-files. *Science* 2001;294:1866-70.
  23. Handschin C, Meyer UA. Induction of drug metabolism: the role of nuclear receptors. *Pharmacol Rev* 2003;55:649-73.
  24. Wang H, LeCluyse EL. Role of orphan nuclear receptors in the regulation of drug-metabolising enzymes. *Clin Pharmacokinet* 2003;42:1331-57.
  25. Xu C, Li CY, Kong AN. Induction of phase I, II and III drug metabolism/transport by xenobiotics. *Arch Pharm Res* 2005;28:249-68.
  26. Maglich JM, Stoltz CM, Goodwin B, Hawkins-Brown D, Moore JT, Kliewer SA. Nuclear pregnane x receptor and constitutive androstane receptor regulate overlapping but distinct sets of genes involved in xenobiotic detoxification. *Mol Pharmacol* 2002;62:638-46.
  27. Moreau A, Vilarem MJ, Maurel P, Pascussi JM. Xenoreceptors CAR and PXR activation and consequences on lipid metabolism, glucose homeostasis, and inflammatory response. *Mol Pharm* 2008;5:35-41.
  28. Pascussi JM, Gerbal-Chaloin S, Duret C, Daujat-Chavanieu M, Vilarem MJ, Maurel P. The tangle of nuclear receptors that controls xenobiotic metabolism and transport: Crosstalk and consequences. *Annu Rev Pharmacol Toxicol* 2008;48:1-32.
  29. Kumarakulasingham M, Rooney PH, Dundas SR, Telfer C, Melvin WT, Curran S, et al. Cytochrome p450 profile of colorectal cancer: Identification of markers of prognosis. *Clin Cancer Res* 2005;11:3758-65.
  30. Pellequer Y, Weissenborn V, Lamprecht A. Decreased drug penetration in inflamed tissue related to changed mucosal metabolism in experimental colitis. *J Pharm Sci* 2007;96:2145-53.
  31. Panwala CM, Jones JC, Viney JL. A novel model of inflammatory bowel disease: mice deficient for the multiple drug resistance gene, *mdr1a*, spontaneously develop colitis. *J Immunol* 1998;161:5733-44.
  32. Langmann T, Moehle C, Mauerer R, Scharl M, Liebisch G, Zahn A, et al. Loss of detoxification in inflammatory bowel disease: Dysregulation of pregnane X receptor target genes. *Gastroenterology* 2004;127:26-40.
  33. Leonard S, Sinensky M. Somatic cell genetics and the study of cholesterol metabolism. *Biochim Biophys Acta* 1988;947:101-12.
  34. Dooley KA, Millinder S, Osborne TF. Sterol regulation of 3-hydroxy-3-methylglutaryl-coenzyme A synthase gene through a direct interaction between sterol regulatory element binding protein and the trimeric CCAAT-binding factor/nuclear factor Y. *J Biol Chem* 1998;273:1349-56.
  35. Mascaro C, Ortíz JA, Ramos MM, Haro D, Hegardt FG. Sterol regulatory element binding protein-mediated effect of fluvastatin on cytosolic 3-hydroxy-3-methylglutaryl-coenzyme A synthase transcription. *Arch Biochem Biophys* 2000;374:286-92.
  36. Yasui Y, Suzuki R, Miyamoto S, Tsukamoto T, Sugie S, Kohno H, et al. A lipophilic statin, pitavastatin, suppresses inflammation-associated mouse colon carcinogenesis. *Int J Cancer* 2007;121:2331-9.
  37. Hegardt FG. Transcriptional regulation of mitochondrial HMG-CoA synthase in the control of ketogenesis. *Biochimie* 1998;80:803-6.
  38. Rodriguez JC, Gil-Gomez G, Hegardt FG, Haro D. Peroxisome proliferator-activated receptor mediates induction of the mitochondrial 3-hydroxy-3-methylglutaryl-CoA synthase gene by fatty acids. *J Biol Chem* 1994;269:18767-72.
  39. Yasui Y, Kim M, Tanaka T. PPAR Ligands for Cancer Chemoprevention. *PPAR Res* 2008;2008:548919.
  40. Kohno H, Suzuki R, Sugie S, Tanaka T. Suppression of colitis-related mouse colon carcinogenesis by a COX-2 inhibitor and PPAR ligands. *BMC Cancer* 2005;5:46.
  41. Tanaka T, Yasui Y, Ishigamori-Suzuki R, Oyama T. Citrus compounds inhibit inflammation- and obesity-related colon carcinogenesis in mice. *Nutr Cancer* 2008;60:70-80.
  42. Powis G, Montfort WR. Properties and biological activities of thioredoxins. *Annu Rev Biophys Biomol Struct* 2001;30:421-55.
  43. Kim M, Miyamoto S, Yasui Y, Oyama T, Murakami A, Tanaka T. Zerubone, a tropical ginger sesquiterpene, inhibits colon and lung carcinogenesis in mice. *Int J Cancer* 2009;124:264-71.
  44. Tanaka T, Yasui Y, Tanaka M, Oyama T, Rahman KM. Melatonin suppresses AOM/DSS-induced large bowel oncogenesis in rats. *Chem Biol Interact* 2009;177:128-36.
  45. Nakamura H, Herzenberg LA, Bai J, Araya S, Kondo N, Nishinaka Y, et al. Circulating thioredoxin suppresses lipopolysaccharide-induced neutrophil chemotaxis. *Proc Natl Acad Sci U S A* 2001;98:15143-8.
  46. Nakamura H, De Rosa SC, Yodoi J, Holmgren A, Ghezzi P, Herzenberg LA. Chronic elevation of plasma thioredoxin: Inhibition of chemotaxis and curtailment of life expectancy in AIDS. *Proc Natl Acad Sci U S A* 2001;98:2688-93.
  47. Sumida Y, Nakashima T, Yoh T, Nakajima Y, Ishikawa H, Mitsuyoshi H, et al. Serum thioredoxin levels as an indicator of oxidative stress in patients with hepatitis C virus infection. *J Hepatol* 2000;33:616-22.
  48. Yoshida S, Katoh T, Tetsuka T, Uno K, Matsui N, Okamoto T. Involvement of thioredoxin in rheumatoid arthritis: Its costimulatory roles in the TNF-alpha-induced production of IL-6 and IL-8 from cultured synovial fibroblasts. *J Immunol* 1999;163:351-8.
  49. Tamaki H, Nakamura H, Nishio A, Nakase H, Ueno S, Uza N, et al. Human thioredoxin-I ameliorates experimental murine colitis in association with suppressed macrophage inhibitory factor production. *Gastroenterology* 2006;131:1110-21.

50. Pawlak G, Helfman DM. Cytoskeletal changes in cell transformation and tumorigenesis. *Curr Opin Genet Dev* 2001;11:41-7.
51. Schleef M, Werner K, Satzger U, Kaupmann K, Jockusch H. Chromosomal localization and genomic cloning of the mouse alpha-tropomyosin gene Tpm-1. *Genomics* 1993;17:519-21.
52. Bakin AV, Safina A, Rinehart C, Daroqui C, Darbary H, Helfman DM. A critical role of tropomyosins in TGF-beta regulation of the actin cytoskeleton and cell motility in epithelial cells. *Mol Biol Cell* 2004;15:4682-94.
53. Das KM, Bajpai M. Tropomyosins in human diseases: ulcerative colitis. *Adv Exp Med Biol* 2008;644:158-67.
54. Geng X, Biancone L, Dai HH, Lin JJ, Yoshizaki N, Dasgupta A, et al. Tropomyosin isoforms in intestinal mucosa: Production of autoantibodies to tropomyosin isoforms in ulcerative colitis. *Gastroenterology* 1998;114:912-22.
55. Wen Z, Fiocchi C. Inflammatory bowel disease: autoimmune or immune-mediated pathogenesis? *Clin Dev Immunol* 2004;11:195-204.



Journal of Carcinogenesis is published for Carcinogenesis Press by Medknow Publications and Media Pvt. Ltd.

Manuscripts submitted to the journal are peer reviewed and published immediately upon acceptance, cited in PubMed and archived on PubMed Central. Your research papers will be available free of charge to the entire biomedical community. Submit your next manuscript to Journal of Carcinogenesis.  
[www.journalonweb.com/jcar/](http://www.journalonweb.com/jcar/)

## AUTHOR'S PROFILE



**Dr. TAKUJI TANAKA, M.D., Ph.D., FIAC**

1978 - 1983: Assistant Professor, Department of Pathology, Gifu University School of Medicine, Japan  
1983 - 1985: Visiting Scientist, Division of Experimental Pathology and Toxicology, Naylor Dana Institute, American Health Foundation, New York, USA

1985 - 1997: Associate Professor, Department of

Pathology, Gifu University School of Medicine, Japan

1997 - : Professor and Chairman, Department of Oncologic Pathology, Kanazawa Medical University, Japan

**Specialty and Present Interest:**

Inflammation and Cancer; Cancer chemoprevention by natural products; Biomarkers of carcinogenesis and cancer chemoprevention; Chemical carcinogenesis

**Memberships for Academic Societies:**

Japanese Cancer Association (1976-; Councilor, 2000-)

Japanese Society of Pathology (1976-; Councilor, 1986-)

Japanese Society of Toxicologic Pathology (1986-)

International Academy of Pathology (1987-)

International Academy of Cytology (MIAC, 1987-; FIAC, 1989-)

American Association for Cancer Research (1989-)

European Association for Cancer Research (1991-)

**Editorial Board:**

Journal of Carcinogenesis (Sr. Editor)

Molecular Carcinogenesis

Chemico-Biological Interactions

Asian Pacific Journal of Cancer Prevention

The Open Toxicology Journal

Journal of Toxicologic Pathology

Japanese Journal of Food Chemistry

Journal of Toxicological Sciences (Associate Editor)

# Enhanced colitis-associated colon carcinogenesis in a novel *Apc* mutant rat

Kazuto Yoshimi,<sup>1</sup> Takuji Tanaka,<sup>2</sup> Akiko Takizawa,<sup>1</sup> Megumi Kato,<sup>3</sup> Masumi Hirabayashi,<sup>3</sup> Tomoji Mashimo,<sup>1</sup> Tadao Serikawa<sup>1</sup> and Takashi Kuramoto<sup>1,4</sup>

<sup>1</sup>Institute of Laboratory Animals, Graduate School of Medicine, Kyoto University, Yoshidakonoe-cho, Sakyo-ku, Kyoto; <sup>2</sup>Department of Oncologic Pathology, Kanazawa Medical University, Uchinada, Ishikawa; <sup>3</sup>National Institute for Physiological Sciences, The Graduate University for Advanced Studies, Okazaki, Japan

(Received May 18, 2009/Revised June 28, 2009/Online publication August 20, 2009)

To establish an efficient rat model for colitis-associated colorectal cancer, azoxymethane and dextran sodium sulfate (AOM/DSS)-induced colon carcinogenesis was applied to a novel adenomatous polyposis coli (*Apc*) mutant, the Kyoto *Apc* Delta (KAD) rat. The KAD rat was derived from ethylnitrosourea mutagenesis and harbors a nonsense mutation in the *Apc* gene (S2523X). The truncated APC of the KAD rat was deduced to lack part of the basic domain, an EB1-binding domain, and a PDZ domain, but retained an intact  $\beta$ -catenin binding region. KAD rats, homozygous for the *Apc* mutation on a genetic background of the F344 rat, showed no spontaneous tumors in the gastrointestinal tract. At 5 weeks of age, male KAD rats were given a single subcutaneous administration of AOM (20 mg/kg, bodyweight). One week later, they were given DSS (2% in drinking water) for 1 week. At week 15, the incidence and multiplicity of colon tumors developed in the KAD rat were remarkably severe compared with those in the F344 rat: 100 versus 50% in incidence and  $10.7 \pm 3.5$  versus  $0.8 \pm 1.0$  in multiplicity. KAD tumors were dominantly distributed in the rectum and distal colon, resembling human colorectal cancer. Accumulation of  $\beta$ -catenin protein and frequent  $\beta$ -catenin mutations were prominent features of KAD colon tumors. To our knowledge, AOM/DSS-induced colon carcinogenesis using the KAD rat is the most efficient to induce colon tumors in the rat, and therefore would be available as an excellent model for human colitis-associated CRC. (*Cancer Sci* 2009; 100: 2022–2027)

Colorectal cancer (CRC) is one of the leading causes of cancer deaths in the world. Globally, the CRC mortality was 639 000 in 2004.<sup>(1)</sup> Chronic inflammation has been identified as a potential risk factor for CRC. Clinical studies have shown that inflammatory bowel disease, such as Crohn's disease<sup>(2)</sup> and ulcerative colitis,<sup>(3)</sup> elevates the risk of CRC.

Animal experiments are assumed to simulate or at least provide plausible pathophysiological mechanisms of various diseases, including cancer and chronic inflammatory disorders. For inflammation-related CRC, a two-stage colitis-related mouse colon carcinogenesis model was recently established.<sup>(4)</sup> In this model, colon carcinogenesis is initiated with carcinogens and then dextran sodium sulfate (DSS), which can induce colonic mucosal inflammation resembling the histopathology of ulcerative colitis, is used as a tumor-promoting agent. Colon carcinogenesis initiated with carcinogens such as azoxymethane (AOM),<sup>(4)</sup> 1,2-dimethylhydrazine (DMH),<sup>(5)</sup> and heterocyclic amines<sup>(6)</sup> is effectively promoted in combination with DSS.

The two-stage colitis-related model has been applied to a rat colon carcinogenesis study. Similar to mice, DSS also promotes DMH-induced<sup>(7)</sup> and AOM-induced<sup>(8)</sup> colon carcinogenesis in the F344 rat. These rat models can be utilized to investigate the pathogenesis of colitis-related colon carcinogenesis and to detect carcinogenesis modifiers.<sup>(7,8)</sup> For more effective colorectal car-

cinogenesis, however, a novel model, in which much more and larger tumors are induced in a shorter experiment period, is required. It would be preferable to obtain a large volume of tumors, sufficient to be identifiable on macroscopic observation, because this would be an advantage in testing chemotherapeutic efficacy of anticancer drugs as well as chemoprevention ability of anti-inflammatory drugs.

One possible idea to enhance the AOM/DSS model is deficiency of the tumor suppressor adenomatous polyposis coli (*Apc*) gene, which plays a significant role in tumor development in the gut,<sup>(9)</sup> for example, AOM enhances colorectal carcinogenesis in *Apc*<sup>min/+</sup> mice that carry a germline mutation in the *Apc* gene and develop multiple polyps in the intestine.<sup>(10)</sup> Furthermore, DSS strongly promotes colorectal carcinogenesis in *Apc*<sup>min/+</sup> mice.<sup>(11)</sup> These findings prompted us to examine AOM/DSS-induced colon carcinogenesis in an *Apc* mutant rat. In the rat, an *Apc*-deficient Pirr rat is available.<sup>(12)</sup> The Pirr rat carries a nonsense mutation in the *Apc* gene and the resultant truncated APC ( $\Delta 1137$ ) lacks the  $\beta$ -catenin binding region. The Pirr rat develops multiple tumors with a distribution between the colon and small intestine. The average number of colonic polyps is  $8 \pm 3$  in Pirr rats aged 4–6 months, and most of them are adenomas. *N*-ethyl-*N*-nitrosourea (ENU) treatment enhances colonic polyps, but it takes more than 7 months to obtain them.<sup>(12)</sup> However, a carcinogenesis test with AOM alone or AOM/DSS has not yet been done in the Pirr rats.

We have recently produced a rat mutant archive consisting of cryopreserved sperm derived from ~5000 ENU-mutagenized male rats and corresponding DNA samples. The mutant archive is estimated to store ~2 million mutations, sufficient to find several mutations in a particular gene of interest.<sup>(13)</sup>

We present here a novel homozygous *Apc* mutant rat strain, the Kyoto *Apc* Delta (KAD) rat, from the rat ENU-mutant archive. KAD rats harbor a nonsense mutation in exon 15 that results in premature termination at codon 2523 of the serine residue of APC protein. KAD rats are viable and show no spontaneous tumors in the small intestine or colorectum. Treatment with AOM/DSS revealed an increased susceptibility of KAD rats to colitis-associated colon carcinogenesis in a 15-week experimental period. Also, the development of colorectal tumors can be tracked by endoscopic observation. AOM/DSS-induced colon carcinogenesis in the KAD rats will provide a novel rat model for investigating colitis-related colon carcinogenesis, identifying xenobiotics with modifying effects, and evaluating anticancer drug candidates.

## Materials and Methods

**Establishment of KAD rat strain.** A total of 1735 DNA samples from ENU-mutagenized F344/NSlc rats from the Kyoto

<sup>4</sup>To whom correspondence should be addressed.  
E-mail: tkuramot@anim.med.kyoto-u.ac.jp

University Rat Mutant Archive (KURMA) were screened with seven sets of primers (Table S1). These primers were designed to amplify exons 9, 11, 14, or 15 of the rat *Apc* gene. Approximately 6.27 Mb of genomic DNA was screened. Rats carrying the *Apc* mutation were recovered by intracytoplasmic sperm injection.<sup>(13)</sup> Male rats carrying the *Apc* mutation were backcrossed five times with female F344/NS1c rats to remove latent mutations induced by ENU.

**Western blotting.** Proteins were prepared from the brainstems of KAD and control F344/NS1c rats at 5 weeks of age. Western blotting and signal detection were carried out as described.<sup>(14)</sup> Antibodies against the N terminus of APC (H-290; Santa Cruz Biotechnology, Santa Cruz, CA, USA), the C terminus of APC (C-20; Santa Cruz Biotechnology), and  $\beta$ -actin (AC-40; Sigma-Aldrich Japan, Tokyo, Japan) were used. Secondary antibodies against rabbit IgG (NA934; GE Healthcare Bio-Sciences, Tokyo, Japan) and mouse IgG (NA931; GE Healthcare Bio-Sciences) were used.

**Carcinogenesis test.** Colon carcinogenic tests were carried out as described.<sup>(4)</sup> Briefly, male KAD rats ( $n = 17$ ) were divided into three experimental and control groups. Group 1 ( $n = 6$ ) was given a single subcutaneous injection of AOM (20 mg/kg body-weight) at 5 weeks of age. Starting 1 week after the AOM injection, animals were given 2% DSS in drinking water for 7 days and then no further treatment for 13 weeks. Groups 2 ( $n = 5$ ) and 3 ( $n = 3$ ) were given AOM alone and DSS alone, respectively. Group 4 ( $n = 3$ ) was untreated. Male F344/NS1c rats

( $n = 6$ ) were treated with AOM followed by DSS (group 5) and were controls of group 1. All rats were maintained under the conditions of humidity ( $50 \pm 10\%$ ), light (14 : 10 h L : D cycle), and temperature ( $24 \pm 2^\circ\text{C}$ ) at the Institute of Laboratory Animals, Graduate School of Medicine, Kyoto University. At 15 weeks after the AOM injection, they were killed by cervical dislocation under anesthesia with isoflurane (Forane; Abbott Japan, Tokyo, Japan). All experimental procedures were approved by the Animal Research Committee of Kyoto University and were carried out according to the Regulation on Animal Experimentation at Kyoto University.

**Histopathology and immunohistochemistry.** At autopsy, the colorectum of the rats was resected, washed with PBS, and opened longitudinally along the main axis. After careful macroscopic inspection, tumors and the colonic mucosa were dissected and processed for histopathological examination with hematoxylin-eosin staining. Immunohistochemical staining of  $\beta$ -catenin was carried out as described previously.<sup>(15)</sup>

**Endoscopic observation and biopsy.** Endoscopic observations were carried out every week after the 8 weeks of the carcinogenesis tests. Anesthesia was administered through the regulated flow of isoflurane vapor (2%) through a nose cone. The colon was flushed with a tap water enema. The endoscope (BF TYPE 3C40; Olympus, Tokyo, Japan) was inserted into the colon and endoscopic images were acquired. A tumor specimen was biopsied under microscopic observation.

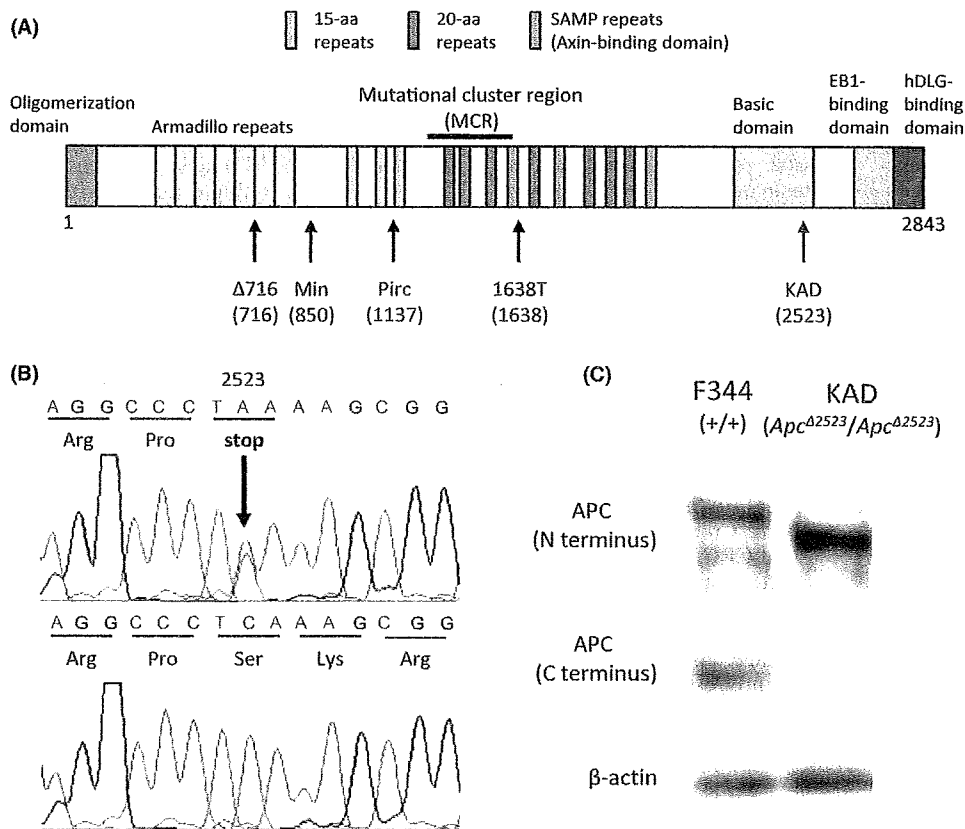


**Fig. 1.** Establishment of the Kyoto *Apc* Delta (KAD) rat strain. (A) Schematic diagram that shows multiple domains of full-length adenomatous polyposis coli (APC). Black arrows indicate orthologous locations of truncating mutations in mouse and rat models. The nonsense mutation in the KAD rat is indicated by a red arrow. (B) Sequence trace of a founder rat showing heterozygosity for C-to-A transversion (arrow) at nucleotide 7621 of the *Apc* gene (upper) compared with wild-type littermates (lower). The mutation generated a premature stop codon (TAA) at the 2523 amino acid position of APC. (C) Western blot analysis of APC in KAD and control F344/NS1c rats. Proteins extracted from the brains of F344 (+/+) and KAD (*Apc* <sup>$\Delta$ 2523</sup>/*Apc* <sup>$\Delta$ 2523</sup>) rats were hybridized with anti-N terminus of APC (top), anti-C terminus of APC (middle) antibodies.  $\beta$ -Actin was used as an internal control (bottom). In KAD rats, smaller APC protein was detected with the anti-N terminus APC antibody than F344 rats, and no signal was detected with the anti-C terminus APC antibody.

**Mutation detection.** Mutations of the  $\beta$ -catenin (*Catnb1*) or K-ras (*Kras*) genes in tumors were screened by direct sequencing. Genomic DNA was extracted from tissues stored in RNAlater (Applied Biosystems, Inc., Carlsbad, CA, USA). PCR primers were designed to amplify mutational hot spots detected in the AOM-induced colon tumors.<sup>(16)</sup> The nucleotide sequences of primers were as follows: r*Catnb1*-F, GCTGACCTCATG-GAGTTGGA and r*Catnb1*-R, GCTACTTGCTCTTGCGTG-AA; r*Kras*-F, TGAATTCAGAATGCCTTAGAGTTTT and r*Kras*-R, GCACCGATGGTTCCTATTA. DNA sequencing was carried out as described previously.<sup>(17)</sup>

## Results

**Establishment of the KAD rat.** A C-to-A point mutation was detected in the DNA archive of KURMA and was predicted to result in premature termination at codon 2523 of the serine residue of the APC protein (Fig. 1A). Rats carrying the mutation were recovered from the corresponding frozen sperm (KURMA sperm archive number: ENU1588) with intracytoplasmic sperm injection.<sup>(13)</sup> The nonsense mutation (c. 7621C > A, p. Ser2523X) was confirmed in recovered animals, which were F<sub>1</sub> hybrids between recipient F344/NSlc and G<sub>1</sub> donor animals (Fig. 1B); we therefore named this allele *Apc* <sup>$\Delta$ 2523</sup>. The deduced APC protein was predicted to lack a part of the basic domain, EB1-binding domain, and PDZ domain (Fig. 1A). Because homozygous Min mice and Pirc rats have been reported to be embryonic lethal,<sup>(12,18)</sup> we crossed *Apc* <sup>$\Delta$ 2523</sup> heterozygous mutants to obtain *Apc* <sup>$\Delta$ 2523</sup> homozygotes. Rats homozygous for *Apc* <sup>$\Delta$ 2523</sup> were viable and survived almost 2 years. We thus designated the *Apc* <sup>$\Delta$ 2523</sup> homozygous strain the KAD rat. Western blot analyses indicated a lack of the C terminus of APC protein in the KAD rat (Fig. 1C). Cellular localization of  $\beta$ -catenin protein was not altered in the colon epithelia of the KAD rat, compared with the F344 rat (data not shown).

**High susceptibility to colitis-associated colon carcinogenesis in the KAD rat.** *Apc* <sup>$\Delta$ 2523</sup> homozygous KAD developed no spontaneous tumors in their gastrointestinal tracts even after 20 months of age. We then tried to induce colon tumors in the KAD rats by administering AOM as a chemical colonic carcinogen and/or DSS as a colitis-inducing agent. The AOM-treated (group 2), DSS-treated (group 3), and non-treated (group 4) KAD rats showed no colon tumors on either macroscopic or microscopic observation. Meanwhile, AOM/DSS-treated KAD rats (group 1) developed multiple colon tumors, of which the incidence, number, and volume could be compared with those of tumors developed in AOM/DSS-treated F344 rats (group 5). Interestingly, the AOM/DSS-treated KAD rats showed a higher incidence of diarrhea than the AOM/DSS-treated F344 rats during a few weeks after the cessation of DSS treatment (Fig. 2).

Macroscopically, all of the AOM/DSS-treated KAD rats showed multiple nodular, polypoid, or caterpillar-like colonic tumors (Fig. 3A), whereas half of the AOM/DSS-treated F344 rats had a few colonic tumors (Fig. 3B). The average number of colorectal tumors in the KAD rat was significantly higher than that of F344 rats ( $9.5 \pm 1.8$  vs  $1.3 \pm 0.8$ ,  $P < 0.0001$ ) (Fig. 4A). The average volume of KAD tumors was not different from that of F344 tumors ( $33.9 \pm 23.0$  mm<sup>3</sup> vs  $10.3 \pm 13.7$  mm<sup>3</sup>,  $P = 0.38$ ). Colon tumors that developed in the KAD rats that received AOM and DSS were distributed more prominently in the rectum ( $4.0 \pm 1.5$ ) and distal colon ( $5.2 \pm 1.7$ ) than in the middle colon ( $0.3 \pm 0.5$ ) (Fig. 4B). No tumors were observed in the proximal colon, cecum, or small intestine.

Microscopically, tumors induced in AOM/DSS-treated KAD rats were diagnosed as tubular adenoma (Fig. 5A), well or moderately differentiated tubular adenocarcinoma (Fig. 5B), or signet-ring cell carcinoma (Fig. S1). The multiplicity of adenoma of the KAD rat was significantly higher than that of the F344 rat

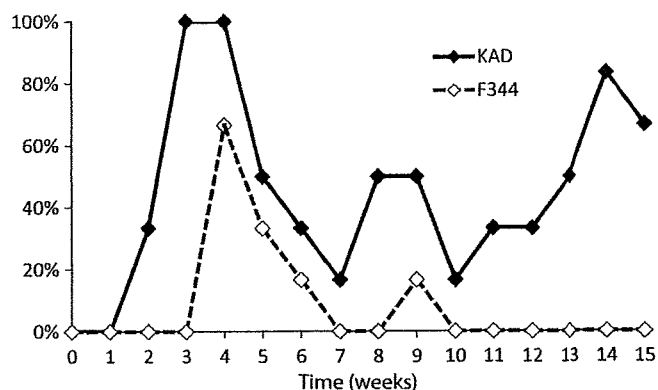


**Fig. 2.** Incidences of diarrhea observed in azoxymethane (AOM)/dextran sodium sulfate (DSS)-treated Kyoto Apc Delta (KAD) and F344 rats. Percentages of rats showing diarrhea in weekly observations are shown. One-week DSS administration is indicated by a grey box. Note that all KAD rats showed diarrhea in week 3, whereas no F344 rats showed diarrhea.

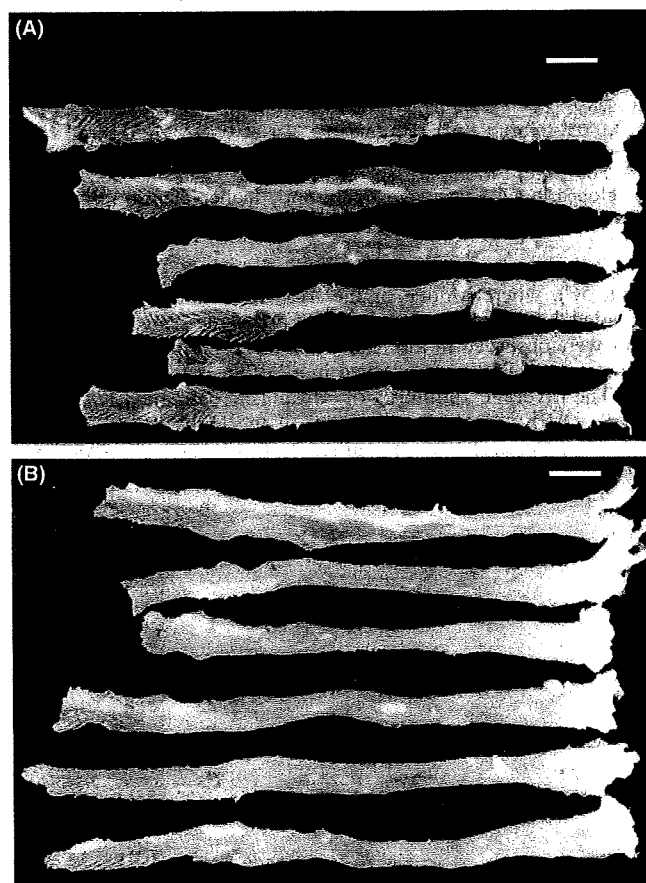


**Fig. 3.** Macroscopic view of large bowels of azoxymethane (AOM)/dextran sodium sulfate (DSS)-treated (A) Kyoto Apc Delta (KAD) and (B) F344 rats. Scale bars = 2 cm.

( $7.7 \pm 2.9$  vs  $0.3 \pm 0.5$ ,  $P < 0.005$ ) (Fig. 4C). The multiplicity of adenocarcinoma of the KAD rat was also significantly higher than that of the F344 rat ( $3.0 \pm 0.9$  vs  $0.5 \pm 0.8$ ,  $P < 0.001$ ) (Fig. 4C). Twenty-two of 64 colon tumors induced in the KAD rats invaded the submucosa, muscularis propria, or serosa

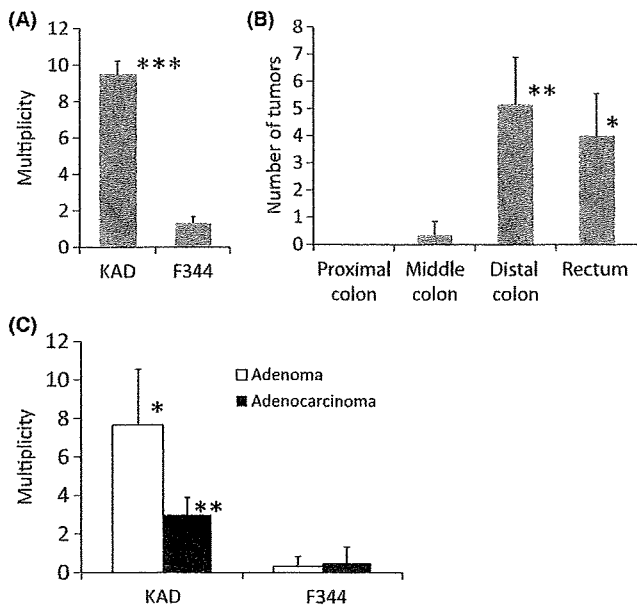


**Fig. 4.** Increased induction of colon tumors in azoxymethane (AOM)/dextran sodium sulfate (DSS)-treated Kyoto Apc Delta (KAD) rats. (A) Multiplicity of tumors observed macroscopically (mean  $\pm$  SD) at week 15. \*\*\* $P < 0.0001$ . (B) Distribution of colon tumors in AOM/DSS-treated KAD rats (mean  $\pm$  SD) at week 15. \*\*Distal colon versus middle colon,  $P < 0.001$ ; \*rectum versus middle colon,  $P < 0.005$ . (C) Multiplicities of adenoma and adenocarcinoma developed in KAD rats were significantly higher than in F344 rats at week 15. \* $P < 0.005$ , \*\* $P < 0.001$ .

(Fig. 5C), whereas none of the five colon tumors in F344 rats invaded the submucosa or deeper. Four signet-ring cell carcinomas were observed in the KAD rats. Apart from colonic tumors, colonic dysplasia was observed in all of the rats in groups 1 and 5. The average number of dysplasias in the KAD rats ( $11.2 \pm 8.0$ ) was greater than that of the F344 rats ( $3.7 \pm 4.1$ ), but the difference was insignificant ( $P = 0.069$ ). No dysplastic lesions developed in groups 2–4.

Altered cellular localization of  $\beta$ -catenin protein is frequently observed in AOM- or AOM/DSS-induced colorectal tumors.<sup>(4,16)</sup> Strong  $\beta$ -catenin expression was seen in the cytoplasm and/or nucleus of adenoma and adenocarcinoma cells (Fig. 5D), which indicated the activation of Wnt signaling in these cells.

**Endoscopic observation and biopsy of colon tumors.** Endoscopic examination was done in the anesthetized KAD rats to determine whether the development of colorectal tumors can be observed without necropsy. We could observe colorectal lesions displaying differences from normal mucosa, including polypoid lesions, as early as the eighth week after AOM administration (Fig. S2A) and could monitor the development of both the number and volume of them during the carcinogenesis test (Fig. S2B). At week 8, the average number of lesions detected by endoscopy was  $3.3 \pm 1.2$ . The number of lesions gradually increased with the experimental period and reached  $17.3 \pm 4.5$  at week 14, which was much higher than that of macroscopic observations. Such a discrepancy might be caused by the disappearance of inflammatory polyps at week 14. The biopsy of a tumor specimen under endoscopic observation was successful and the specimen was diagnosed histopathologically (Fig. S2C).

**Highly frequent mutations of the  $\beta$ -catenin gene but no mutation of the K-ras gene in colon tumors.** Mutation of the  $\beta$ -catenin gene in its glycogen synthase kinase (GSK) 3 $\beta$  phosphorylation consensus motif and K-ras mutation at codon 12 are features of AOM-induced rat colon tumors.<sup>(15,16)</sup> Direct sequencing of PCR products revealed 29 missense mutations in 29 of 39 (74.4%) colon tumors induced by AOM/DSS in KAD rats (Table 1). The mutation spectrum detected in the present study was quite similar to that detected in the AOM-induced rat colon tumors,<sup>(16)</sup> which indicated that a common molecular pathway to initiate colon carcinogenesis was shared in AOM- and AOM/DSS-treated colons. Meanwhile, no K-ras mutation at codon 12 was detected in the 39 colon tumors.

## Discussion

A two-stage colitis-related colon carcinogenesis model provides a powerful tool for the induction of colon tumors.<sup>(7,8)</sup> In the current study, to establish a more efficient colon carcinogenesis model, we produced a novel *Apc*-mutant KAD rat. The

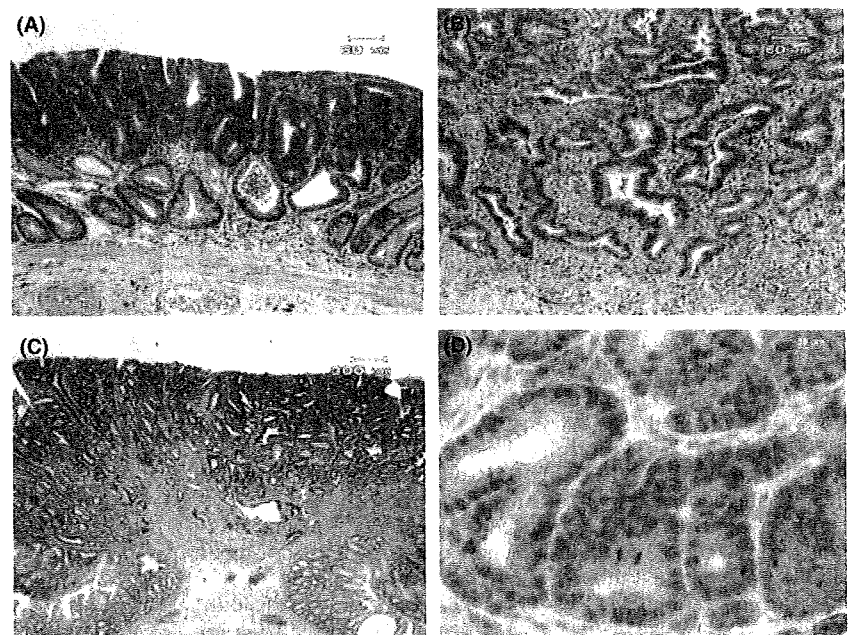


**Fig. 5.** Histopathology of colonic tumors developed in azoxymethane (AOM)/dextran sodium sulfate (DSS)-treated Kyoto Apc Delta (KAD) rats. (A) Tubular adenoma, (B) well-differentiated adenocarcinoma, and (C) moderately differentiated adenocarcinoma invading the submucosa. Hematoxylin–eosin stain. (D)  $\beta$ -Catenin immunohistochemistry in colonic adenocarcinoma.

**Table 1. Mutations in the GSK3 $\beta$  phosphorylation consensus motif of the *Catnrb* gene in colon tumors**

Mutated codon	Base change	Amino acid substitution†	No. mutations detected
32	GAT → AAT	Asp → Asn	8
33	TCT → TTT	Ser → Phe	4
34	GGA → GAA	Gly → Glu	8
37	TCT → TTT	Ser → Phe	2
41	ACC → ATC	Thr → Ile	4
44	CCT → CTT	Pro → Leu	1
45	TCC → TTC	Ser → Phe	2
Total			29

†Serine residues in codons 33, 37, and 45 and the threonine residue in codon 41 are GSK3 $\beta$  phosphorylation sites.

KAD rat harbored a nonsense mutation resulting in the truncated APC protein ( $\Delta 2523$ ), in which the  $\beta$ -catenin-binding region was retained. The KAD rat was viable and showed the normal distribution of  $\beta$ -catenin in colon epithelium and no spontaneous colon tumors. These findings suggested that Wnt signal might not be activated in the non-treated colon epithelium of KAD rats. In humans, a subset of attenuated familial adenomatous polyposis harbors C-terminal-truncated APC mutations such as  $\Delta 2644$  and  $\Delta 2663$ .<sup>(19,20)</sup> The  $\Delta 2644$  APC protein failed to activate Wnt signaling,<sup>(21)</sup> and these patients are rarely related to the occurrence of colonic polyposis, but are responsible for the development of extracolonic lesions, including desmoids, gastric fundic gland hyperplastic polyposis, and osteomas. Although we have not yet observed such extracolonic lesions in the KAD rat, further examinations will allow us to establish the KAD rat as a model for attenuated familial adenomatous polyposis.

The AOM/DSS-treated KAD rat showed colon tumors in 100% incidence, much higher in multiplicity (~10-fold) and more advanced in malignancy than the control F344 rat. These tumors can be obtained in only a short period of 15 weeks. We therefore concluded that AOM/DSS colon carcinogenesis was extensively enhanced in the KAD rat. This carcinogenesis model has also several advantages over the Pirc rat model. The epithelial malignancy of our model is more significant than the Pirc model: our model could induce adenocarcinomas (multiplicity is  $3.0 \pm 0.9$ ), whereas most tumors developed in the colon of the Pirc rat were adenomas. This suggests that we could obtain multiple colon tumors in a shorter period (<15 experimental weeks). Next, we can evaluate the effects of potential carcinogens on colon carcinogenesis more strictly, because KAD are free from spontaneous tumors. Additionally, we can prepare tumor-bearing animals in accordance with our needs, which is a major concern in practical studies. It has been thought that an ideal colon carcinogenesis model would involve not only the efficient induction of tumors but also similar tumor characteristics and good availability for clinical application. The colon tumors developed in the KAD rat showed a predominant distribution in the rectum and distal colon and the accumulation of  $\beta$ -catenin protein, similar to human CRC. Furthermore, the tumors induced were large enough to be observed by endoscopy and biopsied tumor specimens were successfully diagnosed. These findings indicate that the KAD colorectal carcinogenesis model has the potential to mimic clinical operations for human CRC. Our results described here strongly suggest that AOM/DSS-induced colon carcinogenesis with the KAD rat model is ideal and provides an excellent tool to investigate basic and clinical studies on colitis-related CRC. For example, this model enables efficient evaluation of the effects of novel anticancer drugs on tumor regression as well as the effects of anti-inflammatory agents on tumor development. Combination with recently devel-

oped fluorescence probes that image viable cancer cells<sup>(22)</sup> would provide clearer images of tumors and further insights into the pathogenesis of CRC.

In contrast with the AOM/DSS-treated KAD rats, neither AOM-treated nor DSS-treated KAD rats developed colon tumors. It is well known that no colon tumors occurred in the AOM-treated or DSS-treated F344 rats within as short as 15 weeks by the carcinogenesis test.<sup>(7,23,24)</sup> All AOM/DSS-treated KAD rats developed colon tumors. They also had significant diarrhea for a few weeks after cessation of the DSS exposure. These findings indicate that the KAD rat is susceptible to inflammation provoked by a colitis-inducing agent, DSS, and suggest that severe inflammation of the colon epithelia might be involved in the enhancement of colon carcinogenesis in the KAD rat.

DSS-induced colitis occurs mainly in the distal colon,<sup>(25)</sup> which is consistent with the predominant distribution of tumors to the distal colon and rectum in the AOM/DSS-treated KAD rat. Additionally, no K-ras mutation was found in the tumors of AOM/DSS-treated KAD rats. K-ras mutation plays a role as a promoter through enhancing COX-2 and iNOS expression in the presence of inflammatory stimuli.<sup>(16)</sup> However, it is likely that, in our model, DSS enabling the induction of severe inflammation might replace the K-ras mutation. In fact, no mutations of K-ras and a high incidence of substitutions of *Apc* and *p53* genes were found in the colonic tumors induced by a colonic carcinogen, DMH, and a colitis-inducing compound, trinitrobenzene sulfonic acid.<sup>(26)</sup> These findings may support our idea that inflammation provoked by DSS plays an important role in colon carcinogenesis in the KAD rat, and the C terminus of APC, which is lacking in the KAD rat, might be involved in the effect of DSS on tumor development.

The C terminus of APC, which is lacking in the KAD rat, comprises a 321-amino acid polypeptides and contains a part of the basic domain, EB1-binding domain, and PDZ domain,<sup>(27)</sup> by which APC interacts with a variety of cytoskeletal proteins, such as microtubules, the microtubule plus end binding protein (EB1), and the mammalian homolog of Discs large.<sup>(28-30)</sup> With these domains, APC contributes directly and/or indirectly to cell migration, adhesion, chromosome segregation, spindle assembly, and apoptosis in the epithelium of the gut.<sup>(31,32)</sup> In the DSS colitis model, microbiota alteration, epithelial cell toxicity, increased intestinal permeability, and macrophage activation have been proposed as potential pathogenesis mechanisms of colitis.<sup>(33,34)</sup> Although so far there is no direct evidence linking these colitis pathogenesis to the functions of APC domains, it is expected that cell migration or adhesion occurring in response to DSS treatment might be disturbed in KAD by the lack of the C-terminal domains. Alternatively, the responses of epithelial cells to cytokines released from macrophages induced by DSS might be altered. Further pathophysiological analysis of the KAD rat colon epithelium would provide insights into the association of the C terminus of APC with colitis. Importantly, other rodent *Apc* mutant models, such as Min mice and Pirc rats, completely lose all protein interaction sites located in the C-terminal half of the protein. Thus, it is very difficult to determine whether the susceptibility to DSS-induced colitis would result from the effects of the C-terminal or central regions of APC.

In summary, we established an enhanced rat AOM/DSS-induced colitis-related colon carcinogenesis model using a novel *Apc* mutant KAD rat. This colon carcinogenesis model system, to our knowledge, is the most effective in the experimental induction of colon tumors and therefore will contribute greatly to promote experimental studies on the pathogenesis, prevention, and treatment of CRC. The KAD rat also provides insights into the involvement of the C terminus of APC in the development of colitis-related CRC.

## Acknowledgments

The KAD rat strain (NBPR Rat No. 0443), whose official strain name is F344-*Apc*<sup>miKyo</sup> is deposited in the National BioResource Project – Rat in Japan and is available from the Project (<http://www.anim.med.kyoto-u.ac.jp/nbr>). This work was supported in part by a Grant-in-aid for Cancer Research from the Ministry of Health, Labour, and Welfare and

Grants-in-Aid for Scientific Research from the Japan Society for the Promotion of Science (21300153 to TK) and Industrial Technology Research Grant Program in 2008 from New Energy and the Industrial Technology Development Organization (NEDO) of Japan. We are grateful to K. Kumafuji, S. Nakanishi, F. Tagami, and M. Yokoe for their excellent technical assistance.

## References

- 1 WHO. WHO Media Center, Cancer, Fact sheet No. 297. Geneva: WHO, 2009.
- 2 Itzkowitz SH, Yio X. Inflammation and cancer IV. Colorectal cancer in inflammatory bowel disease: the role of inflammation. *Am J Physiol Gastrointest Liver Physiol* 2004; **287**: G7–17.
- 3 Rutter M, Saunders B, Wilkinson K *et al*. Severity of inflammation is a risk factor for colorectal neoplasia in ulcerative colitis. *Gastroenterology* 2004; **126**: 451–9.
- 4 Tanaka T, Kohno H, Suzuki R, Yamada Y, Sugie S, Mori H. A novel inflammation-related mouse colon carcinogenesis model induced by azoxymethane and dextran sodium sulfate. *Cancer Sci* 2003; **94**: 965–73.
- 5 Kohno H, Suzuki R, Sugie S, Tanaka T.  $\beta$ -Catenin mutations in a mouse model of inflammation-related colon carcinogenesis induced by 1,2-dimethylhydrazine and dextran sodium sulfate. *Cancer Sci* 2005; **96**: 69–76.
- 6 Tanaka T, Suzuki R, Kohno H, Sugie S, Takahashi M, Wakabayashi K. Colonic adenocarcinomas rapidly induced by the combined treatment with 2-amino-1-methyl-6-phenylimidazo[4,5-b]pyridine and dextran sodium sulfate in male ICR mice possess  $\beta$ -catenin gene mutations and increases immunoreactivity for  $\beta$ -catenin, cyclooxygenase-2 and inducible nitric oxide synthase. *Carcinogenesis* 2005; **26**: 229–38.
- 7 Onose J, Imai T, Hasumura M, Ueda M, Hirose M. Rapid induction of colorectal tumors in rats initiated with 1,2-dimethylhydrazine followed by dextran sodium sulfate treatment. *Cancer Lett* 2003; **198**: 145–52.
- 8 Tanaka T, Yasui Y, Tanaka M, Tanaka T, Oyama T, Rahuman KMW. Melatonin suppresses AOM/DSS-induced large bowel oncogenesis in rats. *Chem Biol Interact* 2009; **177**: 128–36.
- 9 Kinzler KW, Nilbert MC, Su LK *et al*. Identification of FAP locus genes from chromosome 5q21. *Science* 1991; **253**: 661–5.
- 10 Suzui M, Okuno M, Tanaka T, Nakagama H, Moriwaki H. Enhanced colon carcinogenesis induced by azoxymethane in min mice occurs via a mechanism independent of beta-catenin mutation. *Cancer Lett* 2002; **183**: 31–41.
- 11 Tanaka T, Kohno H, Suzuki R *et al*. Dextran sodium sulfate strongly promotes colorectal carcinogenesis in *Apc*<sup>Min/+</sup> mice: inflammatory stimuli by dextran sodium sulfate results in development of multiple colonic neoplasms. *Int J Cancer* 2006; **118**: 25–34.
- 12 Amos-Landgraf JM, Kwong LN, Kendziorski CM *et al*. A target-selected *Apc*-mutant rat kindred enhances the modeling of familial human colon cancer. *Proc Natl Acad Sci USA* 2007; **104**: 4036–41.
- 13 Mashimo T, Yanagihara K, Tokuda S *et al*. An ENU-induced mutant archive for gene targeting in rats. *Nat Genet* 2008; **40**: 514–15.
- 14 Imai Y, Inoue H, Kataoka A *et al*. Pael receptor is involved in dopamine metabolism in the nigrostriatal system. *Neurosci Res* 2007; **59**: 413–25.
- 15 Takahashi M, Fukuda K, Sugimura T, Wakabayashi K.  $\beta$ -catenin is frequently mutated and demonstrates altered cellular location in azoxymethane-induced rat colon tumors. *Cancer Res* 1998; **58**: 42–6.
- 16 Takahashi M, Wakabayashi K. Gene mutations and altered gene expression in azoxymethane-induced colon carcinogenesis in rodents. *Cancer Sci* 2004; **95**: 475–80.
- 17 Gohma H, Kuramoto T, Kuwamura M *et al*. WTC deafness Kyoto (*dftk*): a rat model for extensive investigations of *Kcnql* functions. *Physiol Genomics* 2006; **24**: 198–206.
- 18 Moser AR, Pitot HC, Dove WF. A dominant mutation that predisposes to multiple intestinal neoplasia in the mouse. *Science* 1990; **247**: 322–4.
- 19 Couture J, Mitri A, Lagace R *et al*. A germline mutation at the extreme 3' end of the APC gene results in a severe desmoid phenotype and is associated with overexpression of beta-catenin in the desmoid tumor. *Clin Genet* 2000; **57**: 205–12.
- 20 Matsubara N, Isozaki H, Tanaka N. The farthest 3' distal end APC mutation identified in attenuated adenomatous polyposis coli with extracolonic manifestations. *Dis Colon Rectum* 2000; **43**: 720–1.
- 21 Morin PJ, Sparks AB, Korinek V *et al*. Activation of  $\beta$ -catenin-Tcf signaling in colon cancer by mutations in  $\beta$ -catenin or APC. *Science* 1997; **275**: 1787–90.
- 22 Urano Y, Asanuma D, Hama Y *et al*. Selective molecular imaging of viable cancer cells with pH-activatable fluorescence probes. *Nat Med* 2009; **15**: 104–9.
- 23 Ghirardi M, Nascimbeni R, Villanacci V, Fontana MG, Di Betta E, Salemi B. Azoxymethane-induced aberrant crypt foci and colorectal tumors in F344 rats: sequential analysis of growth. *Eur Surg Res* 1999; **31**: 272–80.
- 24 Paulsen JE, Loberg EM, Olstorn HB, Knutsen H, Steffensen IL, Alexander J. Flat dysplastic aberrant crypt foci are related to tumorigenesis in the colon of azoxymethane-treated rat. *Cancer Res* 2005; **65**: 121–9.
- 25 Okayasu I, Hatakeyama S, Yamada M, Ohkusa T, Inagaki Y, Nakaya R. A novel method in the induction of reliable experimental acute and chronic ulcerative colitis in mice. *Gastroenterology* 1990; **98**: 694–702.
- 26 Santiago C, Pagan B, Isidro AA, Appleyard CB. Prolonged chronic inflammation progresses to dysplasia in a novel rat model of colitis-associated colon cancer. *Cancer Res* 2007; **67**: 10 766–73.
- 27 Aoki K, Taketo MM. Adenomatous polyposis coli (APC): a multi-functional tumor suppressor gene. *J Cell Sci* 2007; **120**: 3327–35.
- 28 Munemitsu S, Souza B, Muller O, Albert I, Rubinfeld B, Polakis P. The APC gene product associates with microtubules *in vivo* and promotes their assembly *in vitro*. *Cancer Res* 1994; **54**: 3676–81.
- 29 Su LK, Burrell M, Hill DE *et al*. APC binds to the novel protein EB1. *Cancer Res* 1995; **55**: 2972–7.
- 30 Matsumine A, Ogai A, Senda T *et al*. Binding of APC to the human homolog of the *Drosophila* discs large tumor suppressor protein. *Science* 1996; **272**: 1020–3.
- 31 McCartney BM, Nathke IS. Cell regulation by the Apc protein: Apc as master regulator of epithelia. *Curr Opin Cell Biol* 2008; **20**: 186–93.
- 32 Hanson CA, Miller JR. Non-traditional roles for the adenomatous polyposis coli (APC) tumor suppressor protein. *Gene* 2005; **361**: 1–12.
- 33 Boismenu R, Chen Y. Insights from mouse models of colitis. *J Leukoc Biol* 2000; **67**: 267–78.
- 34 Elson CO, Cong Y, McCracken VJ, Dimmitt RA, Lorenz RG, Weaver CT. Experimental models of inflammatory bowel disease reveal innate, adaptive, and regulatory mechanisms of host dialogue with the microbiota. *Immunol Rev* 2005; **206**: 260–76.

## Supporting Information

Additional supporting information may be found in the online version of this article:

**Fig. S1.** Signet-ring cell carcinoma observed in the colon of AOM/DSS-treated KAD rats. Four signet-ring cell carcinomas were observed in AOM/DSS-treated KAD rats (group 1).

**Fig. S2.** Endoscopic observation of KAD colon tumors and biopsy. (A) Endoscopic image of a colon tumor in a KAD rat at week 11. Bleeding from this tumor was found (arrow). (B) Development of colorectal lesions in KAD rats treated with AOM and DSS (group 1). The average numbers of lesions observed by endoscopy were plotted. (C) Microscopic view of a specimen biopsied under endoscopic observation. The specimen was diagnosed as well-differentiated adenocarcinoma. Bar: 60  $\mu$ m.

**Video S1.** Biopsy of a colorectal tumor induced by AOM/DSS two-stage colitis-related carcinogenesis in the KAD rat.

**Table S1.** Primers used in screening for *Apc* mutation in KURMA ENU-mutagenized DNA archives.

Please note: Wiley-Blackwell are not responsible for the content or functionality of any supporting materials supplied by the authors. Any queries (other than missing material) should be directed to the corresponding author for the article.

## Dietary Tricin Suppresses Inflammation-Related Colon Carcinogenesis in Male Crj: CD-1 Mice

Takeru Oyama,<sup>1</sup> Yumiko Yasui,<sup>1</sup> Shigeyuki Sugie,<sup>1</sup> Mamoru Koketsu,<sup>2</sup> Kunitomo Watanabe<sup>3</sup> and Takuji Tanaka<sup>1,4</sup>

### Abstract

The flavone 4',5,7-trihydroxy-3',5'-dimethoxyflavone (tricin) present in rice, oats, barley, and wheat exhibits antigrowth activity in several human cancer cell lines and anti-inflammatory potential. However, the chemopreventive activity has not yet been elucidated in preclinical animal models of colorectal cancer. This study was designed to determine whether dietary tricin exerts inflammation-associated colon carcinogenesis induced by azoxymethane and dextran sulfate sodium in mice. Male Crj: CD-1 mice were initiated with a single i.p. injection of azoxymethane (10 mg/kg body weight) and followed by a 1-week exposure to dextran sulfate sodium (1.5%, w/v) in drinking water to induce colonic neoplasms. They were then given the experimental diet containing 50 or 250 ppm tricin. The experiment was terminated at week 18 to determine the chemopreventive efficacy of tricin. In addition, the effects of dietary tricin on the expression of several inflammatory cytokines, including tumor necrosis factor (TNF)- $\alpha$ , were assayed. The development of colonic adenomas and adenocarcinomas was significantly reduced by feeding with 50 and 250 ppm tricin, respectively. Dietary tricin also significantly reduced the proliferation of adenocarcinoma cells as well as the numbers of mitoses/anaphase bridging in adenocarcinoma cells. The dietary administration with tricin significantly inhibited the expression of TNF- $\alpha$  in the nonlesional crypts. Our findings that dietary tricin inhibits inflammation-related mouse colon carcinogenesis by suppressing the expression of TNF- $\alpha$  in the nonlesional crypts and the proliferation of adenocarcinomas suggest a potential use of tricin for clinical trials of colorectal cancer chemoprevention.

Cancer mortality rates in the developed countries have increased throughout this century, and has been already the leading cause of death in some Western countries (1, 2). Great advances have been made in the pharmacologic-based treatment of malignant epithelial malignancies. There has also been a marked increase in the understanding of cell and molecular mechanisms underlying a variety of carcinogenic processes (3). However, therapeutic options for advanced neoplastic disease remain limited. This lack of treatment alter-

natives may be due to the large number of genetic and molecular alterations associated with advanced neoplasms that contribute to the maintenance of neoplastic progression.

The chemopreventive approach to inhibit cancer development and progression is highly attractive. Practical limitations may exist with respect to developing novel and effective chemopreventive agents through the use of appropriate animal models for preclinical evaluation of candidate chemopreventive agents (4). Some herbal and botanical products that contain flavonoids are likely to possess cancer preventive activities (5). A diet rich in fruits and vegetables has long been suggested to correlate with a reduced risk of certain epithelial malignancies, including cancers in the colon, lung, prostate, oral cavity, and breast (5-7). A number of agents have been reported to be candidate *chemo-inhibitors* of cancer development in various tissues, including colon. Among these agents are the flavonoids, a group of phenolic compounds with structural formula of diphenyl-propane and secondary metabolites produced by plants (5, 8, 9).

4',5,7-Trihydroxy-3',5'-dimethoxyflavone (tricin; Fig. 1A) is a flavone, a subgroup of the flavonoid group, which is found in rice, oats, barley, and wheat (10). Although the physiologic function of tricin in plants is not well defined, the compound is thought to be produced by the plant during times of environmental stress or pathogenic attack (11) and exert potential allelopathic effects (12). Evidence for the biological activity of tricin in rodents has recently been reported. These biological activities

**Authors' Affiliations:** <sup>1</sup>Department of Oncologic Pathology, Kanazawa Medical University, Ishikawa, Japan; <sup>2</sup>Divisions of Instrumental Analysis and <sup>3</sup>Anaerobe Research, Life Science Research Center, Gifu University; and <sup>4</sup>The Tohoku Cytopathology Institute: Cancer Research and Prevention, Gifu, Japan  
Received 4/3/09; revised 7/7/09; accepted 7/22/09; published OnlineFirst 11/24/09.

**Grant support:** Grant-in-Aid for Cancer Research, for the Third-Term Comprehensive 10-Year Strategy for Cancer Control from the Ministry of Health, Labour and Welfare of Japan; Grants-in-Aid grant nos. 18592076 (T. Tanaka), 17015016 (T. Tanaka), and 18880030 (Y. Yasui) for Scientific Research from the Ministry of Education, Culture, Sports, Science and Technology of Japan; and grant H2008-12 (T. Tanaka) for the Project Research from the High-Technology Center of Kanazawa Medical University.

**Note:** Supplementary data for this article are available at Cancer Prevention Research Online (<http://cancerprevres.aacrjournals.org/>).

**Requests for reprints:** Takuji Tanaka, Department of Oncologic Pathology, Kanazawa Medical University, 1-1 Daigaku, Uchinada, Ishikawa 920-0293, Japan. Phone: 81-76-218-8116; Fax: 81-76-286-6926; E-mail: takutt@kanazawa-med.ac.jp.

©2009 American Association for Cancer Research.  
doi:10.1158/1940-6207.CAPR-09-0061